

Stress Analysis of Steam-Methane Reformer Tube

by

Cik Suhana Binti Hassan

Dissertation submitted in partial fulfilment of
the requirements for the
Bachelor of Engineering (Hons)
(Mechanical Engineering)

DECEMBER 2008

Universiti Teknologi PETRONAS

Bandar Seri Iskandar

31750 Tronoh

Perak Darul Ridzuan

CERTIFICATION OF APPROVAL

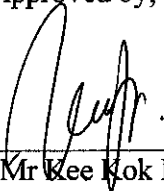
Stress Analysis of Steam-Methane Reformer Tube

by

Cik Suhana Binti Hassan

A project dissertation submitted to the
Mechanical Engineering Programme
Universiti Teknologi PETRONAS
in partial fulfilment of the requirement for the
BACHELOR OF ENGINEERING (Hons)
(MECHANICAL ENGINEERING)

Approved by,



(Mr Kee Kok Eng)

UNIVERSITI TEKNOLOGI PETRONAS

TRONOH, PERAK

July 2008

CERTIFICATION OF ORIGINALITY

This is to certify that I am responsible for the work submitted in this project, that the original work is my own except as specified in the references and acknowledgements, and that the original work contained herein have not been undertaken or done by unspecified sources or persons.

A handwritten signature in black ink, appearing to be 'Cik Suhana Binti Hassan', is written above a solid horizontal line.

CIK SUHANA BINTI HASSAN

ABSTRACT

Reformer tubes are designed to last at least 100,000 hours (11.4 years) of operation, but frequently, some of the tubes in the furnace fail prematurely. Most of the failures occur due to the high temperature and pressure developed within the tubes. Thus, the use of Finite Element Analysis (FEA) software to model, simulate and draw meaningful conclusion from the actual process conditions of the reformer tubes can reveal important information regarding the mechanical and thermal stress response. The main objective of this project is to simulate the combined stress and temperature profiles developed within the reformer tube. This project involves modeling the mechanical and thermal loadings present in the tube as well as simulating the stress distribution across the tube's thickness and length. FEA using ANSYS utilized to analyze stress and temperature profile of the tube. Literature review of reformer tube has been performed and data needed has been identified. Stresses have been computed using ANSYS and verified with theoretical value. It has been seen that the temperature difference across the tube length resulted from the non-uniform heat transfer coefficient can be considerable causing high thermal stresses. Maximum von mises stress equal to 142.61 MPa developed at the inner surface of the entrance region. The stress then compared with the tensile strength of the tube and it is showed that the tube is able to sustain the stress without fracture.

ACKNOWLEDGEMENT

Alhamdulillah, praises to The Almighty Allah for blessing me with the strength and health towards completing this project entitled “Thermal Stress Analysis on Steam-methane Reformer Tube” and also for the ability to fulfill the requirement for completing this project which are reports, poster and presentations.

First of all, I would like to express my deepest appreciation to my supervisor, Mr Kee Kok Eng for giving me the opportunity to work under his supervision as well as for the tremendous job he has done in monitoring and guiding throughout this project.

I would like to express my gratitude to all those who gave me the possibility to complete this project. I am deeply indebted to my co-supervisor, Dr Azmi Bin Abdul Wahab and all general assistance (GA) whose help, stimulating suggestions and encouragement in all the time of my internship.

I gratefully acknowledge Mr Rahmat Iskandar for sharing knowledge with me and for the constructive criticisms and suggestions as well as the enthusiastic support.

Deeply thanks to the Final Year Project coordinators, Dr Puteri Seri Melur, Puan Rosmawati and Professor Vijay whom deeply involve in providing guidelines and scheduling in order to make this final year project successful.

Last but not least, many thanks to all the family, friends and everyone who had involved either directly or indirectly in completing this project.

TABLE OF CONTENTS

CERTIFICATION OF APPROVAL.	ii
CERTIFICATION OF ORIGINALITY.	iii
ABSTRACT.	iv
ACKNOWLEDGEMENTS.	v
TABLE OF CONTENTS.	vi
LIST OF FIGURES..	vii
LIST OF TABLES.	
CHAPTER 1:	INTRODUCTION.	1
	1.1 Project Background.	1
	1.2 Problem Statement.	1
	1.3 Objectives.	4
	1.4 Scope of Work.	4
CHAPTER 2:	LITERATURE REVIEW.	5
	2.2 Reviews on Past Research Work.	5
	2.2.1 Steam-gas Reformer's Process.	5
	2.2.2 Properties of Reformer Tube.	6
	2.3 Heat Transfer Principle.	10
	2.4 Finite Element Analysis (FEA).	11
CHAPTER 3:	METHODOLOGY.	12
	3.1 Procedure Identification.	12
	3.2 FYP Important Milestone.	13
	3.3 Gantt Chart.	13
	3.4 ANSYS General Procedure.	13
	3.4.1 Coupled Analysis in ANSYS.	15
	3.5 Procedures.	16

CHAPTER 4:	RESULT AND DISCUSSION.	. . .	17
	4.1 Data Gathering and Analysis.	. . .	17
	4.1.1 Temperature and Pressure Profile.	. . .	17
	4.2 Project/Problem Description.	. . .	19
	4.3 Theoretical Calculation.	. . .	22
	4.3.1 Thermal Stresses.	. . .	22
	4.3.2 Stresses Due to Internal Pressure.	. . .	22
	4.3.3 Effective Stress..	. . .	23
	4.4 Results.	. . .	24
	4.4.1 Stress Distribution Across the Tube's Thickness.	. . .	24
	4.4.2 Stress Distribution Across the Tube's Length.	. . .	32
	4.5 Comparison with Yield Strength of the Material..		38
CHAPTER 5:	CONCLUSION.	. . .	40
REFERENCES.	41
APPENDICES.	44

LIST OF FIGURES

Figure 1	Photographs of nine failed tubes.	3
Figure 2	Typical axial profiles of skin tube, inner wall and process temperatures, process pressure and heat flux along a steam reformer catalyst tube	8
Figure 3	Total elastic stresses on loading of a reformer tube	9
Figure 4	Steady state stress distribution in a reformer tube.	9
Figure 5	Schematic flow diagram of the project.	10
Figure 6	Procedures of using ANSYS for the project.	16
Figure 7	Temperature and pressure profile of the sample.	18
Figure 8	Simplified scheme of an industrial steam reformer.	19
Figure 9	Problem sketch.	21
Figure 10	Representative FEA model illustrate the mesh	21
Figure 11	Description of the model.	21
Figure 12	Representative model showing paths of results taken.	22
Figure 13	Graph of stress distribution at the entrance region.	26
Figure 14	Contour plot of stress distribution at the entrance region	27
Figure 15	Graph of stress distribution at the middle of the tube.	29
Figure 16	Graph of stress distribution at the tube's process exit.	31
Figure 17	Contour plot of Von Mises stress distribution at the exit.	31
Figure 18	Stress distribution on the inner surface across the tube's length	34
Figure 19	Stress distribution on the outer surface across the tube's length	37
Figure 20	Yield strength and max. Von Mises stress versus temperature.	39

LIST OF TABLES

Table 1	Dimensional measurement of failed reformer tubes.	3
Table 2	Metallurgy developments of reformer tube.	6
Table 3	Material and mechanical properties of the tube	17
Table 4	Data of temperature and pressure across the length of tube.	18
Table 5	Geometric properties and loadings of the tube.	19
Table 6	Stresses across the tube's thickness at the entrance region.	22
Table 7	Result comparison between theoretical and actual Von Mises stress at the entrance region	25
Table 8	Stresses distribution across the tube's thickness at the middle.	27
Table 9	Result comparison between theoretical and actual Von Mises stress at the middle region.	28
Table 10	Stress distribution across the tube's thickness at the exit	29
Table 11	Result comparison between theoretical and actual Von Mises stress at the exit region.	30
Table 12	Stress distribution on the inner surface across the tube's length	32
Table 13	Result comparison between theoretical and actual Von Mises stress on the inner surface.	33
Table 14	Stress distribution on the outer surface across the tube's length	35
Table 15	Result comparison between theoretical and actual Von Mises stress on the outer surface.	36
Table 16	Yield strength of the reformer tube	38
Table 17	Comparison of max. Von Mises stress with yield strength.	38

CHAPTER 1

INTRODUCTION

1.1 Project Background

The steam reforming furnaces are used to convert a process gas mixture (or simply called feedstock) of hydrocarbons and steam into hydrocarbon-rich gases which are used in the manufacture of methanol, ammonia etc. In all cases however, the feedstock is passed through reformer tubes which are filled with catalyst and, since heat is required to maintain the important endothermic reactions, the outsides of the reformer tubes are heated by burners in a large fire box, to temperatures in the range 875-1000°C. Simultaneously, the feedstock is maintained at a high internal pressure in the tube [1].

Finite element analysis using ANSYS will be employed in this project. Finite element analysis (FEA) is a computer simulation technique used in engineering analysis. A common use of FEA is for the determination of stresses and displacements in mechanical objects and systems. Finite element software will be used to compute stresses caused by pressure, thermal and mechanical loadings.

1.2 Problem Statement

Reformer tubes used in steam methane reforming furnace operate under very aggressive conditions and are designed to withstand the combination of high metal temperatures, internal pressure and corrosion for an operational life of 8-12 years, depending upon the type of furnace and the method of operation. They are subjected to high temperature and pressure conditions in varying manners. In these conditions, the

material properties are highly dependent on the temperature profile which in turn influences the stress response of the tube.

The temperature distribution in a part can cause thermal stress effects (stresses caused by thermal expansion or contraction of the material). Examples of this phenomena include interference fit processes (also called shrink or press fit, where parts are mated by heating one part and keeping the other part cool for easy assembly) and creep (permanent deformation resulting from prolonged application of a stress below the elastic limit, such as the behavior of metals exposed to elevated temperatures over time) [2].

As an example, reformer tubes from a fertilizer plant made of modified HK 40 steel which failed after 4 years service were investigated for failure mechanism and life evaluation. Analysis revealed that longitudinal cracks found in the tubes were caused by overheating because of inadequate feed flow caused by the choking of damaged catalyst. At the time of failure the reformer was being started up with only 60 burners firing in the reformer. The gas in the catalyst tubes was mainly hydrogen and steam at a pressure of 3 kg/cm² only. A total of seven tubes ruptured in the bottom portion in one corner of the radiant chamber. Another two tubes ruptured away from this zone in the bottom portion. The rupture was longitudinal. These tubes had been operation for 2 years. Dimensional measurements of the failed reformer tubes are shown in Table 1 (see Fig. 1). [3]

Analysis on stress distribution of reformer tube is chosen to be the subject for this project due to its important application industry. Reformer tubes are extremely important component in reformer which is at the heart of any methanol plant and represents the largest capital expenditure unit operation and also is the largest energy user on the plant. The purpose of this project is to conduct a detailed simulation of the reformer to determine the pressure and temperature profiles axially along the tube. From this information, the stress being applied to the tube can be calculated and then, using the allowable stress-temperature data for the chosen material, the design temperature for the tube can be calculated. Thus, the combined stress and temperature profiles

developed within the tube are important data for the assessment of the material's integrity.

Table 1: Dimensional measurement of the failed reformer tubes and their measured crack lengths [3].

Tube no.	Crack length (mm)	Max. OD (mm)	Crack length (mm)	L (mm) ^a	Fig tail diameter (mm)
144	850	169	19	470	42.4
143	570	160.7	12.4	625	42.4
142	880	159	16	630	42.5
141	630	158	17	870	42.1
140	620	158.6	13	860	42.2
139	630	157.4	10	870	42.2
138	500	156.9	11.5	280	42.2
131	400	154.9	10	1220	42.2
121	600	155.2	-	1100	42.1



Fig.1: Photograph of nine failed tubes, as received [3]

1.3 Objectives

The main goal of this project is to simulate the combined stress and temperature profiles developed within the reformer tube. For these complex loadings, numerical analysis can be employed to simulate the conditions.

The objectives are:

- To model the mechanical and thermal loadings present within the tube.
- To simulate stress distribution across the tube's thickness and length.
- To draw a meaningful conclusion based on the numerical analysis on completion of the project.

1.4 Scope of Work

This is a computational simulation project where the stresses and temperature profile of reformer tube will be simulated. Computer simulation is the discipline of designing a model of an actual or theoretical physical system, executing the model on a digital computer, and analyzing the execution output. Therefore the scopes of work for this project are:

Scope of work:

- 1) Perform literature review on reformer tube as well as finite element analysis techniques.
- 2) Find the raw data (temperature profile and loadings) for reformer tube.
- 3) Model the mechanical and thermal loadings present in the tube.
- 4) Simulate the stress and temperature distribution across the tube's thickness and length.
- 5) Analyze and conclude the results.

CHAPTER 2

LITERATURE REVIEW

2.1 Reviews on Past Research Works

The evaluation of stresses in a thick cylinder pressure vessel such as reformer tube is important for principal design consideration. Therefore, many investigators have directed their effort to study the pressure vessels in order to predict the required working capacity. Sinha [4] used the finite element method to analyze thermal stresses and temperature distribution in a hollow thick cylinder subjected to steady state heat flow in the radial direction.

The study of pressure vessels subjected to both internal pressure and temperature was carried out by many researches. Naga [5] presented a close insight into stress analysis and optimization of both thick walled impermeable and permeable cylinders under the combined effect of stationary temperature and pressure gradients. Gunha [6] calculated the radial and hoop stresses conditions of a specified location within the wall of a cylindrical component configuration. Considerable loads were induced by constant pressure, steady state logarithmic temperature gradients and centrifugal body force [7].

2.2 Theories

2.2.1 Steam-gas Reformer's Process

The steam-gas reformer is a common but critical piece of equipment in ammonia and methanol plants. In most plants, methane is used as feedstock. It reacts with steam in catalyst-packed tubes at high temperature. The process is highly endothermic. The

tubes have inside diameters of 60-120 mm (2.5 in.) and are 10-14 m (33-46 ft.) long. The pressure is 15-30 bar (218-435 psi) and the temperature between 900 to 1000°C (1652-1832°F). The tube wall thickness ranges from 8 to 20 mm (0.31-0.79 in.) depending on the tube diameter, temperature and pressure. Excess steam is used to reduce the formation of carbon. The reforming reactions are favored by high temperature but retarded by high pressure [8].

2.2.2 Properties of Reformer Tube

Due to prolonged exposure to high temperature, the microstructure of the material is subjected to degradation. For example, in the early stages, precipitation of carbides occurs. Following this, there is reduction in strength and embrittlement due to coalescence and coarsening of the carbides. Further degradation might lead to creep cavitations damage, micro cracking and final propagation of macro-cracks leading to catastrophic failure.

Through researches that have been made, it is known that there has been a great deal of development in the area of tube metallurgy in the last 50 years, first with the introduction of centrifugally cast tubes in the 1950s, moving through to the introduction of HK40 in the early 1960s and then on to the HP modified tubes in the mid-1970s and finally the HP micro-alloys in the mid-1980's [9]. The following table illustrates the development of the metallurgy with time.

Table 2: Metallurgy developments of reformer tube [9].

Date	Common name	Cr %	Ni %	Nb %	Others	Relative strength
1960s	HK40	25	20	-	-	1.0
1970s	IN51	25	24	1	-	1.4
Mid-1970s	HP Mod	25	35	1	-	1.9
Mid-1980s	HP Micro-alloy	25	35	1	Ti, Zr, W, Cs	2.2

Traditionally, HK40 alloy were used in the construction of reformer tube due to its creep rupture strength. With moderately high temperature strength, oxidation resistance and carburization resistance the alloy is used in a wide variety of industrial applications [10]. IN51 is the same as HK 40 but with enhanced high temperature resistance up to 1025 C. The microstructural of IN519 has improved the creep strength and ductility of the material [11]. Common versions of HP grade alloy are the HP40 which have improved high temperature strengths, and thus better resistant to thermal stresses and thermal cycling plus superior performance in both oxidizing and carburizing atmospheres [11]. It has much higher creep-rupture strength, carburization resistance and oxidation resistance than HK 40 alloy and consequently is used at higher service temperatures [10]. Current trend, the preferred tube materials are the so-called 'microalloys' which further enhance the high temperature properties of the reformer alloy [11].

Figure 2 schematically presents the process conditions along the length of a catalyst tube. Process gas and steam typically enter each reformer tube between 450 and 500°C and exit at about 850°C, with a slight pressure drop down the length of the tube. The tube metal skin temperature varies along the length of each tube and reflects the design of the unit, the firing configuration and the required process conditions. The thermal through-wall temperature gradient is greatest towards the inlet end of a tube while the effective creep temperature (mean wall temperature) is highest towards the outlet end of the tube [12].

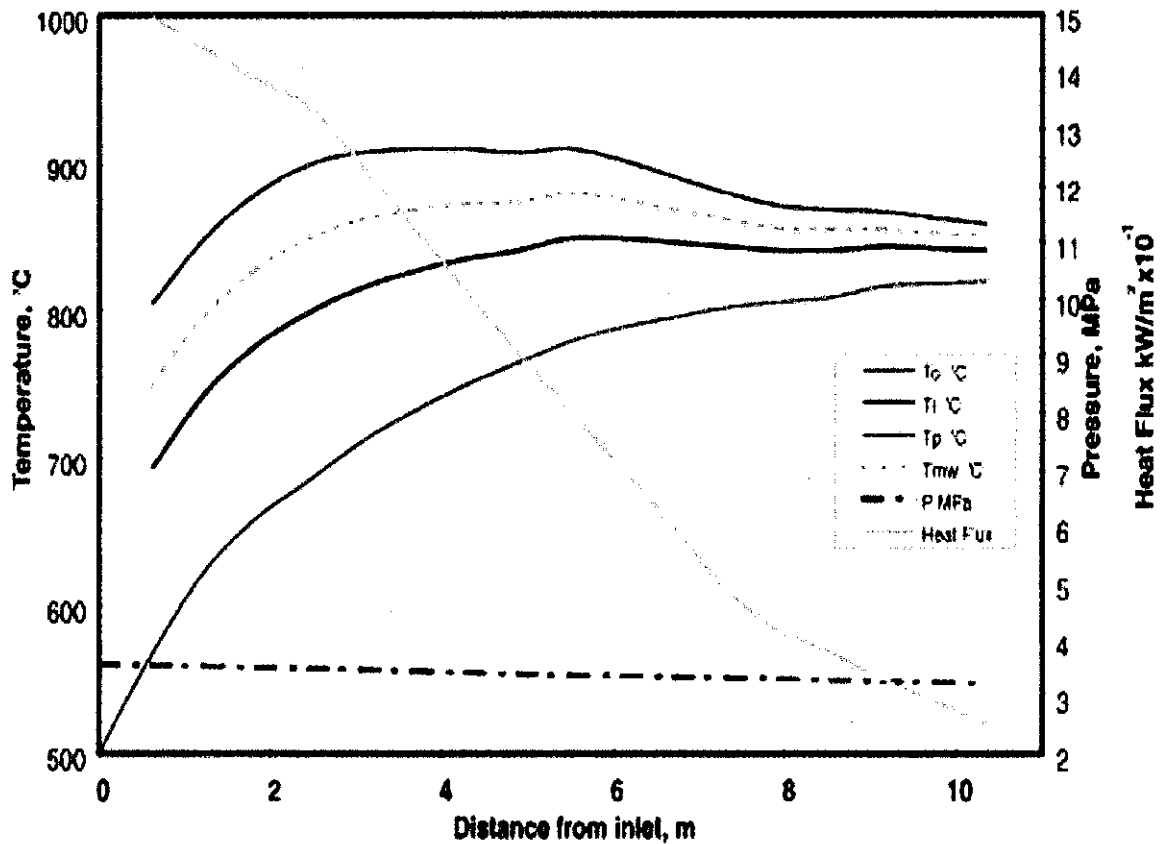


Fig. 2: Typical axial profiles of tube skin, inner wall and process temperatures, process pressure and heat flux along a steam reformer catalyst tube [12].

Solutions for the elastic and steady state stress profiles through the wall of a tube subject to thermal and pressure loadings are well established. Fig. 3 and Fig. 4 show the principal stress components on elastic loading and after a steady state have been achieved, for a typical reformer tube. The difference in magnitude between the elastic and steady state stresses is noteworthy. Modelling the evolution from the former state to the latter, even for a simple axisymmetric component, requires numerical solution [12].

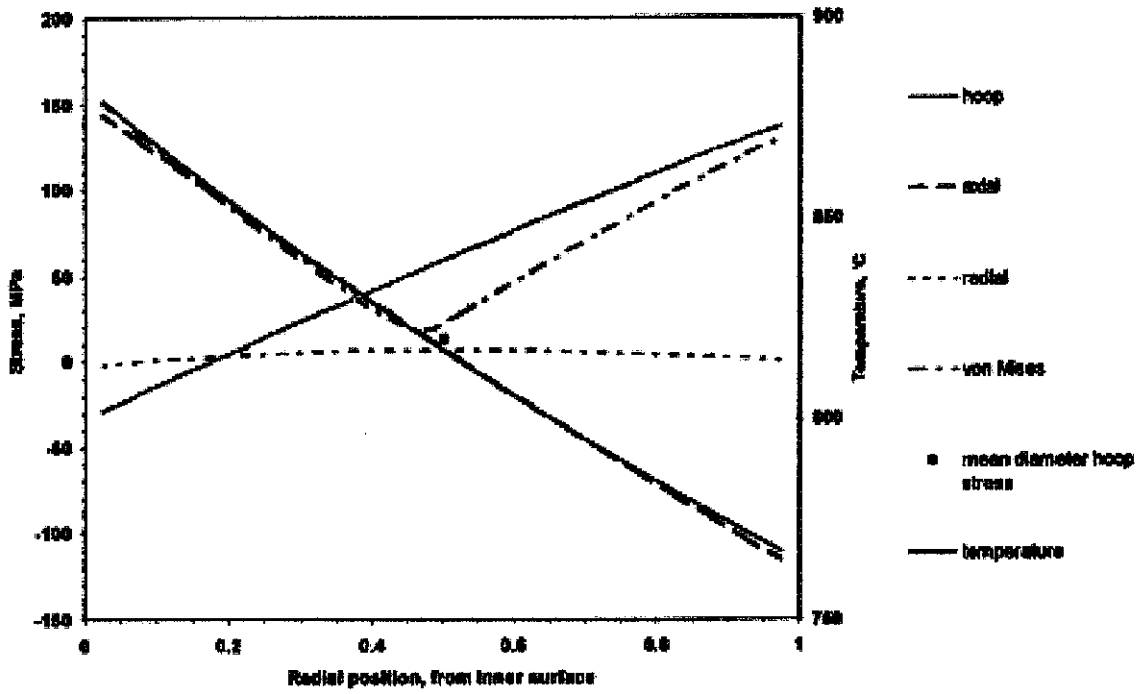


Fig. 3: Total elastic stresses on loading of a reformer catalyst tube [12].

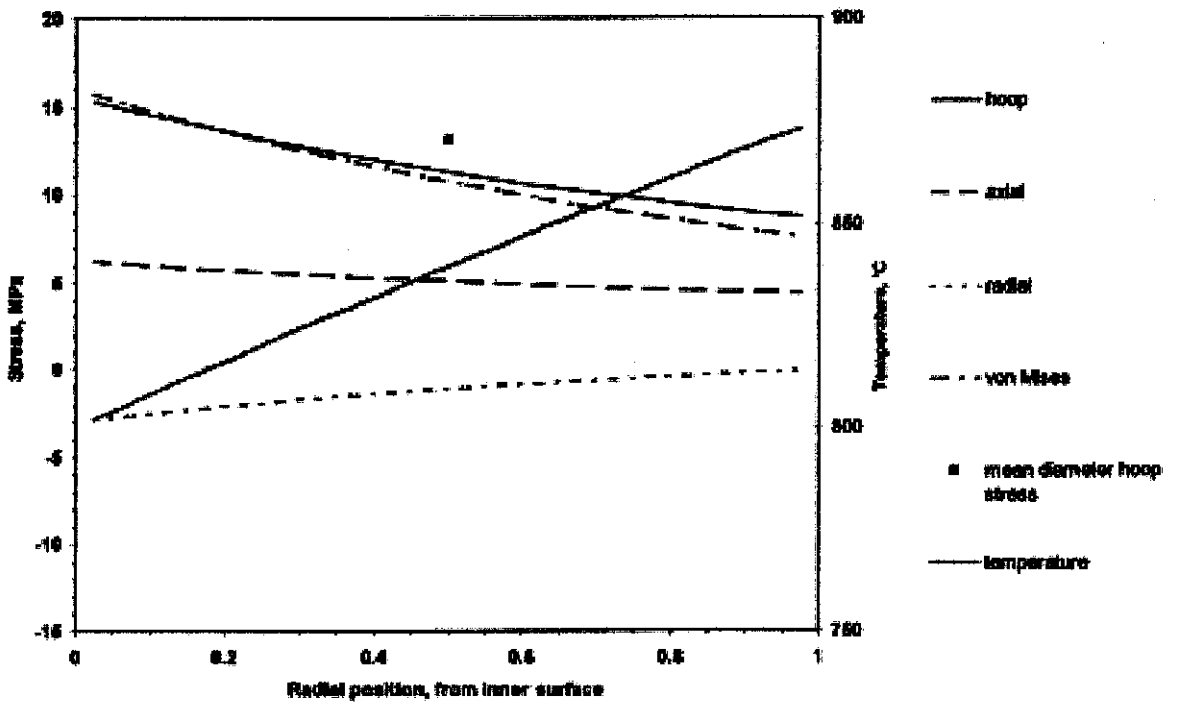


Fig. 4: Steady state stress distribution in a reformer catalyst tube [12].

2.3 Heat Transfer Principle

The reforming reaction is endothermic. In conventional reformers, the necessary heat for the reaction is supplied from the environment outside the tubes usually by a combination of radiation and convection to the outer side of the reformer tube. The heat is transferred to the inner side of the tube by heat conduction through the tube wall and is transferred to the gas phase by convection. Finally, the heat is transferred from the gas phase to the catalyst pellet by convection [14].

Heat conduction or thermal conduction is the spontaneous transfer of thermal energy through matter, from a region of higher temperature to a region of lower temperature, and acts to equalize temperature differences. Thermal energy, in the form of continuous random motion of the particles of the matter, is transferred by the same coulomb forces that act to support the structure of matter, so can be said to move by physical contact between the particles.

Convection is one of the major modes of heat transfer and mass transfer. In fluids, convective heat and mass transfer take place through both diffusion – the random Brownian motion of individual particles in the fluid – and by advection, in which matter or heat is transported by the larger-scale motion of currents in the fluid. In the context of heat and mass transfer, the term "convection" is used to refer to the sum of advective and diffusive transfer.

Radiation is the electromagnetic waves that directly transport energy through space. Radiation, as used in physics, is energy in the form of waves or moving subatomic particles emitted by an atom or other body as it changes from a higher energy state to a lower energy state [15].

2.4 Finite Element Analysis (FEA)

FEA uses a complex system of points called nodes which make a grid called a mesh. This mesh is programmed to contain the material and structural properties which define how the structure will react to certain loading conditions. Nodes are assigned at a certain density throughout the material depending on the anticipated stress levels of a particular area. Regions which will receive large amounts of stress usually have a higher node density than those which experience little or no stress. Points of interest may consist of: fracture point of previously tested material, fillets, corners, complex detail, and high stress areas. The mesh acts like a spider web in that from each node, there extends a mesh element to each of the adjacent nodes. This web of vectors is what carries the material properties to the object, creating many elements [13]. However, batch file method will be used in this project. ANSYS batch file is a series of command listing. Tasks to be performed in ANSYS will be done by inputting the appropriate commands. All of the commands are recorded in the input history file.

CHAPTER 3 METHODOLOGY

3.1 Procedure Identification

Procedures to be employed in this project are clearly illustrated in Figure 5 below.

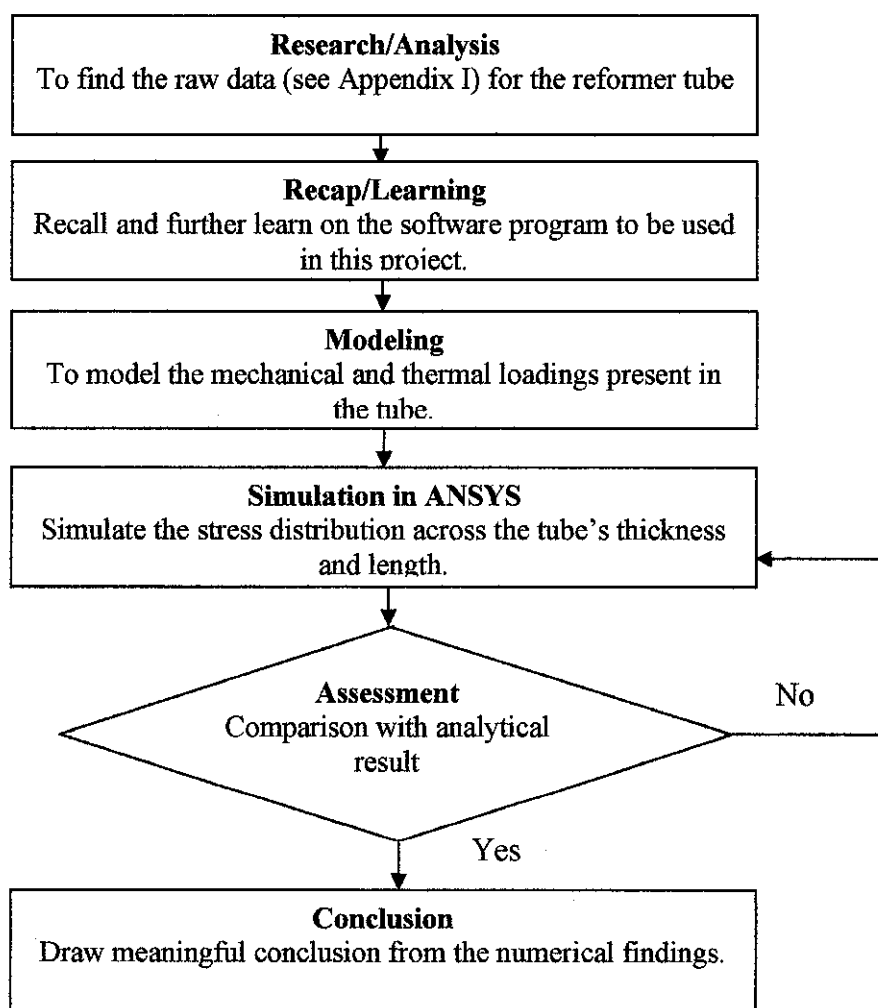


Fig. 5: Schematic flow diagram of the project

3.2 FYP Important Milestone

15th February 2008: Submission of Preliminary Report

17th – 21st March 2008: Submission of FYP I Progress Report and Seminar.

Week of 21st April 2008: Submission of Interim Report and Oral.

15th August 2008: Submission of Progress Report 1

8th – 12th September 2008: Submission of Progress Report 2 and Seminar.

10th October 2008: Poster Exposition.

17th October 2008: Dissertation Draft and Final Presentation.

10th December 2008: Hardbound Dissertation.

3.3 Gantt Chart

Refer Appendix II for the Gantt charts.

3.4 ANSYS General Procedure

ANSYS will be used in this project. ANSYS is a comprehensive general-purpose finite element computer program that contains over 100,000 lines of code. ANSYS is capable of performing static, dynamic, heat transfer, fluid flow and electromagnetism analyses.

There are three stages that are used most frequently in ANSYS:

I. Preprocessor

The preprocessor contains the list of commands needed to create a finite element model:

- a. Define element types and options
- b. Define element real constants
- c. Define material properties

At this point, physical properties of the material will be defined such as modulus of elasticity, Poisson's ratio, thermal conductivity and etc...

- d. Create model geometry
- e. Define meshing objects
- f. Mesh the object created

II. Processor

The next step involves applying appropriate boundary conditions and the proper loading. The solution processor has the commands that allow applying boundary conditions and loads. It includes:

- a. For structural problems: displacements, forces, pressures, temperature for thermal expansion
- b. For thermal problems: temperatures, heat transfer rates, convection surfaces, internal heat generation

III. Postprocessor

Postprocessors are available for review the result [17].

- a. Enter the general postprocessor and read in the results
- b. Define paths
- c. List the solution
- d. Plot the stresses on every paths defined
- e. Exit the ANSYS program

3.4.1 Coupled Analysis in ANSYS

A sequentially coupled physics analysis is the combination of analyses from different engineering disciplines which interact to solve a global engineering problem. When the input of one physics analysis depends on the results from another analysis, the analyses

are coupled. The term sequentially coupled physics refers to solving one physics simulation after another. Results from one analysis become loads for the next analysis.

The complete set of boundary conditions and loads consists of the following:

- Base physics loads, which are not a function of other physics analyses. Such loads also are called nominal boundary conditions.
- Coupled loads, which are results of the other physics simulation [17].

Thus, each different physics environment must be constructed separately so they can be used to determine the coupled physics solution. By creating the geometry in the first physical environment, and using it with any following coupled environments, the geometry is kept constant [18].

The temperature distribution in a part can cause thermal stress effects (stresses caused by thermal expansion or contraction of the material). Since thermal distribution in a reformer tube gives big influence on the stress response, coupled field analysis can be used to evaluate the thermal stress of the tube. For this case, geometry will be created in the Thermal Environment, where the thermal effects will be applied. Although the geometry remains constant, the element types can change. For instance, thermal elements are required to determine the stress in the reformer tube. Thermal stress effects of the reformer tube can be simulated by coupling a heat transfer analysis (steady-state). The process consists of two basic steps:

1. A heat transfer analysis is performed to determine the temperature distribution
2. The temperature results are directly input as loads in a structural analysis to determine the stress and displacement caused by the temperature load

3.5 Procedures

The basic procedures for the physics environment approach in this problem are shown in Figure 6 below:

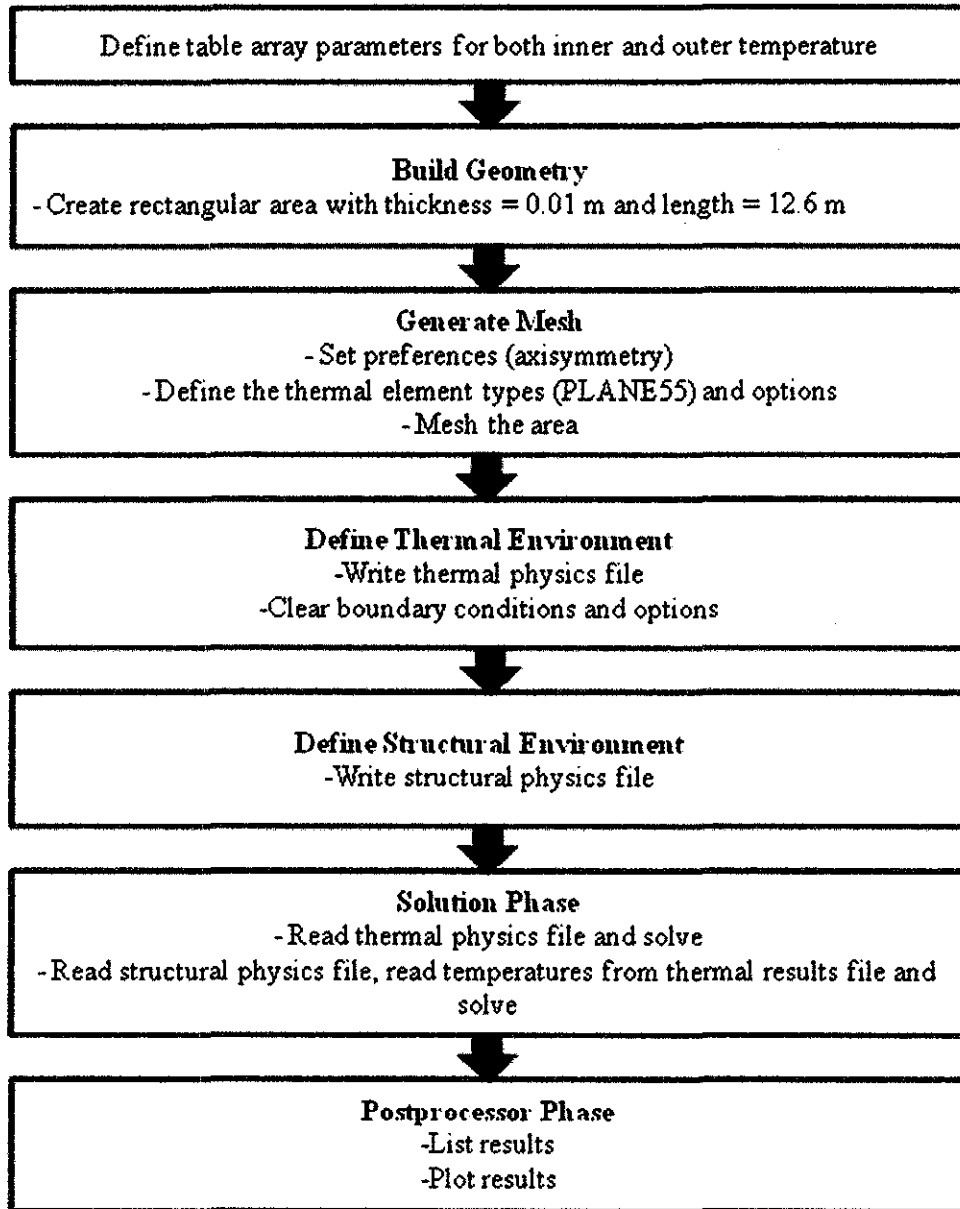


Fig. 6: Procedures of using ANSYS for the project

Refer Appendix III for procedures of using ANSYS's graphical user interface (GUI) and Appendix IV for input listing (batch file) of this project.

CHAPTER 4

RESULT AND DISCUSSION

4.1 Data Gathering and Analysis

4.1.1 Temperature and Pressure Profile

All data to be used in this project referred to the thesis based on a single reformer tube that was retired after 90,000 hours service at Methanex Kitimat plant in British Columbia, Canada. The tube material is Schmidt-Clemens Centralloy® CA4852-Micro centrifugally cast austenitic stainless steel with physical and mechanical properties as showed in Table 3 below (Appendix 1):

Table 3: Material and mechanical properties of the tube

Temperature, K	293	473	673	873	1073	1273	1373
Young Modulus, N/m²	170e9	163e9	145e9	127e9	109e9	96e9	92e9
Thermal conductivity, W/m.K	14.6	14.6	14.6	14.6	14.6	14.6	14.6
Coefficient of linear expansion, 10⁻⁶/°C	15	15.8	16	16.3	17	18.5	19
Poisson's ratio (ν)	0.3	0.3	0.3	0.3	0.3	0.3	0.3
Density (kg/m³)	8000	8000	8000	8000	8000	8000	8000

The tube experienced non-uniform temperature distribution across the tube length of 12.6 m resulted from the non-uniform heat transfer coefficient. A temperature and pressure profile of the reformer tube has been tabulated using Microsoft Excel based on the data from the failed sample (see Table 4). Profiles for the inner and outer wall temperatures and the internal pressure for this ex-service tube are shown in Figure 7.

Table 4: Data of temperature and pressure across the length of the reformer tube [11].

Distance Down Tube m	Outer Wall Temperature °C	Inner Wall Temperature °C	ΔT °C	Internal Pressure Mpa
0	656.2	576.2	80	2.239
0.588	722.9	650.2	72.7	2.2194
1.176	782.8	713.2	69.6	2.1998
1.765	823.2	752.5	70.7	2.1802
2.353	847.1	774.1	73	2.1606
2.941	862.8	789.8	73	2.1411
3.529	873.1	803.5	69.6	2.1215
4	877	812.1	64.9	2.1058
4.641	878	820.4	57.6	2.0845
5.281	877.1	826.6	50.5	2.0631
5.922	876.2	832.2	44	2.0418
6.05	876.1	833.3	42.8	2.0375
6.671	876.2	838.8	37.4	2.0169
7.291	877	844.2	32.8	1.9962
7.912	878.5	849.8	28.7	1.9755
8.533	880.5	855.2	25.3	1.9549
9.154	882.9	860.6	22.3	1.9342
9.774	885.4	865.9	19.5	1.9135
10.271	883.8	867.6	16.2	1.897
10.843	882.1	869.1	13	1.878
11.414	883.3	872	11.3	1.859
11.986	885.5	875.4	10.1	1.84
12.1	886	876	10	1.8361
12.6	885.9	875.9	10	1.8199

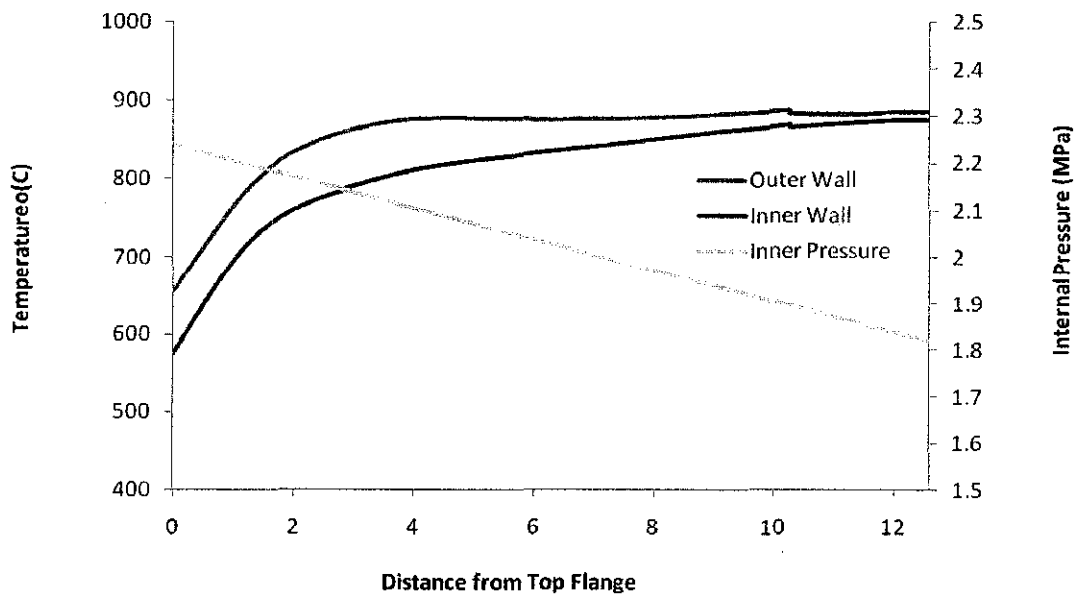


Fig. 7: Temperature and pressure profile of the sample

Conventional steam reformers are furnaces containing tubes filled with reforming catalyst. Figure 8 shows a schematic lateral temperature profile inside a single reformer tube.

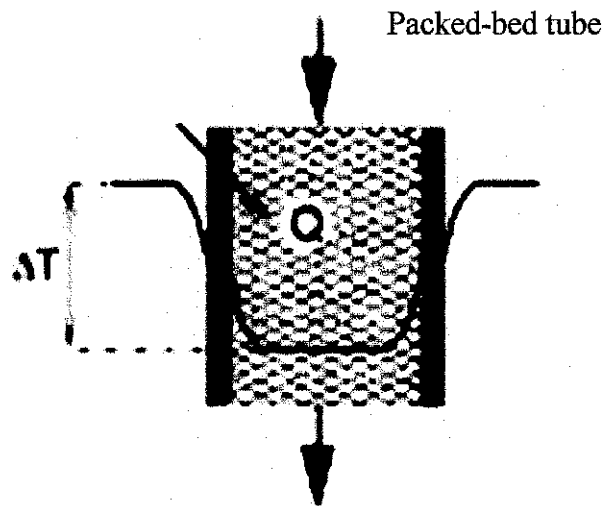


Fig. 8: Simplified scheme of an industrial steam reformer. Lateral temperature profile inside a single reformer tube [16].

4.2 Project/Problem Description

This is an axisymmetric analysis with geometric properties and loadings showed in Table 5 below. Axisymmetric analysis is a problem in which the geometry, loadings, boundary conditions and materials are symmetric with respect to an axis is one that can be solved as an axisymmetric problem instead of as a three dimensional problem.

Table 5: Geometric properties and loadings of the tube

Geometric Properties	Loadings
Inner radius = 0.125 m	T_i = Refer Table 3
Outer radius = 0.135 m	T_o = Refer Table 3
Length = 12.6 m	Internal Pressure: Refer Table 3

A reformer tube has temperature and pressure distribution according to Table 3 and Figure 7 showed above on its inner and outer surface. Figure 7 schematically presents

the process conditions along the length of the reformer tube that retire after 90000 hours of services at the Methanex Kitimat plant in British Columbia, Canada. The process typically enter the reformer tube between 576.2 and 656.2°C and exit at about 875.9 to 885.9°C, with a slight pressure drop down from 2.239 MPa to 1.8911 MPa across the length of the tube. The tube metal skin temperature varies along the length of each tube and reflects the design of the unit, the firing configuration and the required process conditions. The thermal through-wall temperature gradient is greatest at the tube inlet.

An axisymmetric model is chosen to demonstrate the thermal-stress analysis. An eight-node quadrilateral element type PLANE55 use to model the thermal response while element type PLANE42 use to model the structural response. With element edge length of 0.0004, there are 819026 nodes and 787500 elements produced in ANSYS.

The thermal model is constructed first. Temperature constraints are applied to the inner and outer surface. The structural model is constructed next. Pressure constraints applied to the inner surface. Constraints are applied to simulate generalized plane strain conditions.

The process basically requires creation of all the necessary environments, which are basically the preprocessing portions for each environment, and write them to memory. Then in the solution phase they can be combined to solve the coupled analysis. In the preprocessor phase, thermal analysis is identified as field #1, assigning the thermal element type to that field. In a similar fashion, the structural analysis is identified as field #2 with the structural element type assigned to that field. Field file names are assigned which will be used in the naming of the results files. Field #1 named as thermal while field #2 named as structural. Since this is a static analysis, the time is set to 1.0 in the solution phase. The solution is then performed.

The following assumptions are taken into consideration during the analysis:

1. The cylinders are assumed to free to expand, generalized plane strain.
2. There is no source of heat generation within the cylinder thickness.

Figure 9, 10 and 11 below show the sketch of the problem.

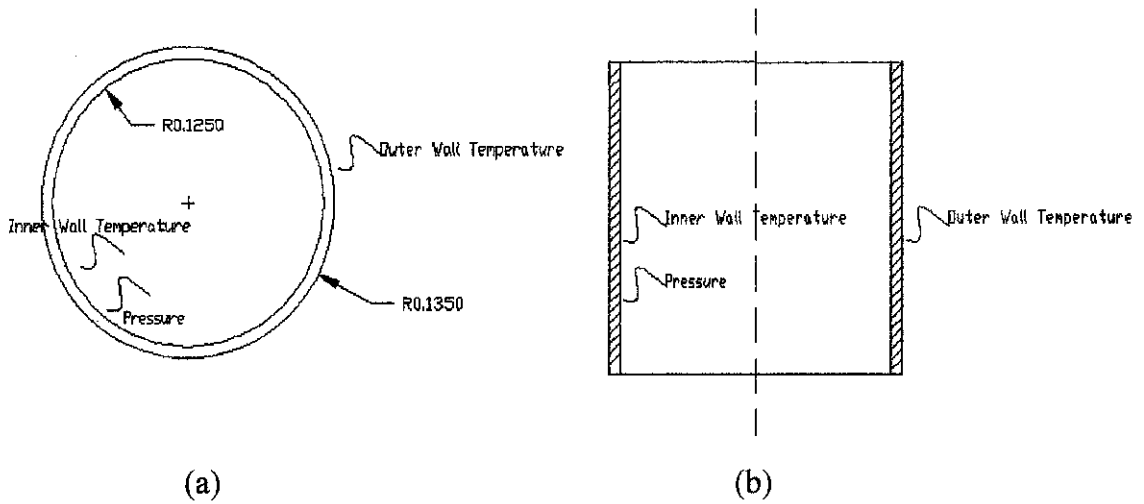


Figure 9: Problem sketch, (a) top view and (b) side view

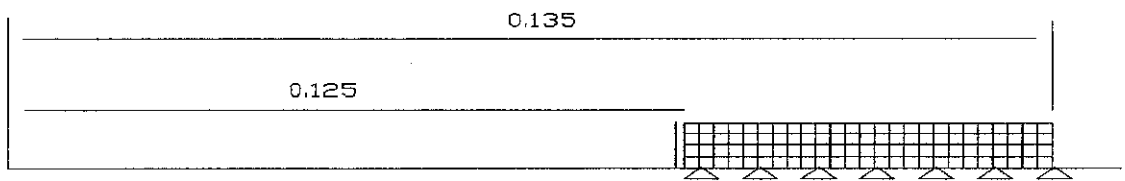


Fig 10: Representative Finite Element Model illustrates the thermal and structural mesh.

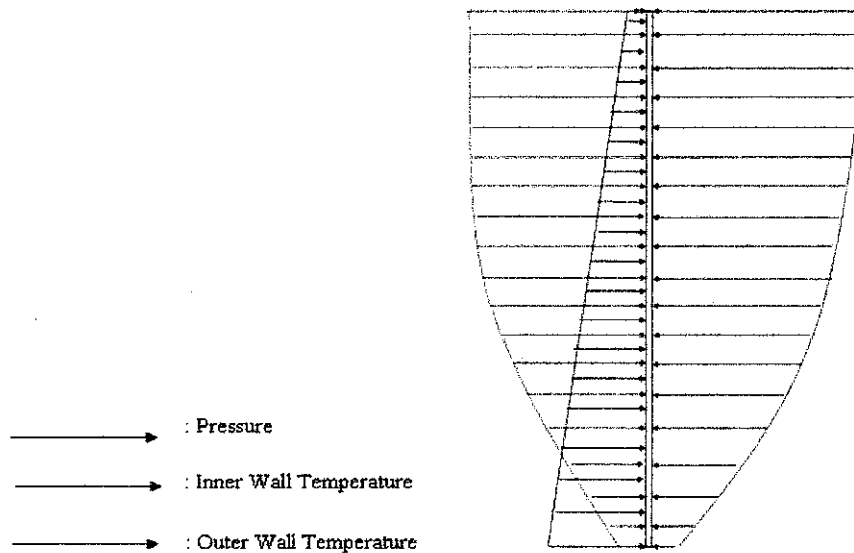


Figure 11: Description of the model

4.3 Theoretical Calculation

All results obtained in ANSYS were compared with theoretical calculations.

4.3.1 Thermal Stresses

Assuming a steady heat flux through the wall with α_T , E and ν also being constant across the wall, the hoop, radial and axial, thermal stresses can be approximated by:

$$\text{hoop stress: } \sigma_{hT} = \frac{\alpha_T E (T_i - T_o)}{2(1-\nu)} \left[\frac{1 - \ln\left(\frac{r_o}{r}\right) - \left(\frac{r_o}{r}\right)^2 + 1}{\ln\left(\frac{r_o}{r_i}\right) - \left(\frac{r_o}{r_i}\right)^2 - 1} \right]$$

$$\text{radial stress: } \sigma_{rT} = \frac{\alpha_T E (T_i - T_o)}{2(1-\nu)} \left[\frac{-\ln\frac{r_o}{r} + \left(\frac{r_o}{r}\right)^2 - 1}{\ln\frac{r_o}{r_i} + \left(\frac{r_o}{r_i}\right)^2 - 1} \right]$$

$$\text{axial stress: } \sigma_{aT} = \frac{\alpha_T E (T_i - T_o)}{2(1-\nu)} \left[\frac{1 - 2\ln\frac{r_o}{r} - \frac{2}{\left(\frac{r_o}{r_i}\right)^2 - 1}}{\ln\frac{r_o}{r_i} + \left(\frac{r_o}{r_i}\right)^2 - 1} \right]$$

4.3.2 Stresses Due to Internal Pressure

Lame's Equations: hoop, radial and axial stresses due to internal pressure p in a long thick-walled cylinder:

$$\text{hoop stress: } \sigma_{rp} = \frac{pr_i^2}{r_o^2 - r_i^2} \left[1 + \frac{r_o^2}{r^2} \right]$$

$$\text{radial stress: } \sigma_{rp} = \frac{pr_i^2}{r_o^2 - r_i^2} \left[1 - \frac{r_o^2}{r^2} \right]$$

$$\text{axial stress: } \sigma_{rp} = \frac{pr_i^2}{r_o^2 - r_i^2}$$

4.3.3 Effective Stress

Effective stress calculated using the Von Mises criterion as follows:

$$\text{Von Mises, } \bar{\sigma}_H = \frac{1}{\sqrt{2}} \sqrt{(\sigma_1 - \sigma_2)^2 + (\sigma_2 - \sigma_3)^2 + (\sigma_3 - \sigma_1)^2}$$

Where;

$$\sigma_1 = \sigma_{hT} + \sigma_{hp}$$

$$\sigma_2 = \sigma_{rT} + \sigma_{rp}$$

$$\sigma_3 = \sigma_{aT} + \sigma_{ap}$$

Variables:

α_T	=	coefficient of thermal expansion
E	=	modulus of elasticity
ν	=	Poisson's ratio
r_i	=	tube internal radius
r_o	=	tube external radius
T_i	=	inside wall temperature
T_o	=	outside wall temperature
r	=	radial distance to point of interest
p	=	internal pressure

Refer Appendix V for example of theoretical calculation and Appendix VI for the rest of theoretical results.

4.4 Results

Following abbreviations were used;

U_X = radial displacement (m)

S_X = radial stress (Pa)

S_Y = axial stress (Pa)

S_Z = hoop stress (Pa)

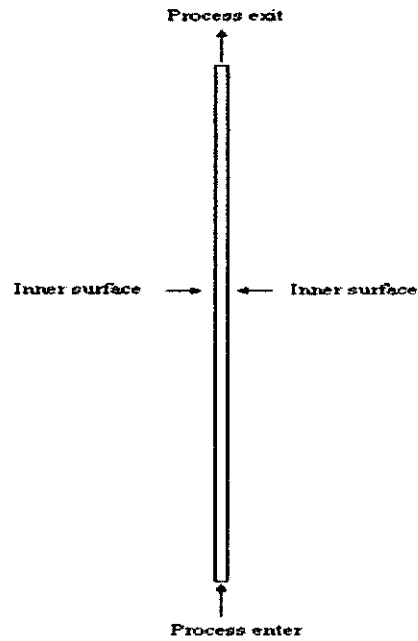


Figure 12: Representative model of the tube showing paths where results are taken.

4.4.1 Stress distribution across the tube's thickness

1. At the process entry side

Table 6: Stresses across the tube's thickness at entrance region.

```

PRINT ALONG PATH DEFINED BY LPATH COMMAND.  DSYS= 0
***** PATH VARIABLE SUMMARY *****

```

S	XG	U_X	S_X	S_Y	S_Z	S_EQV
0.0000	0.12500	-0.51121E-03	-0.17180E+07	0.12793E+09	0.15178E+09	0.14307E+09
0.50000E-03	0.12550	-0.51396E-03	-0.13397E+07	0.11415E+09	0.13753E+09	0.12878E+09
0.10000E-02	0.12600	-0.51665E-03	-0.81950E+06	0.10087E+09	0.12392E+09	0.11496E+09
0.15000E-02	0.12650	-0.51928E-03	-0.36366E+06	0.87678E+08	0.11049E+09	0.10139E+09
0.20000E-02	0.12700	-0.52185E-03	36718.	0.74587E+08	0.97244E+08	0.88093E+08
0.25000E-02	0.12750	-0.52434E-03	0.37160E+06	0.61652E+08	0.84218E+08	0.75149E+08
0.30000E-02	0.12800	-0.52678E-03	0.61609E+06	0.48969E+08	0.71453E+08	0.62696E+08
0.35000E-02	0.12850	-0.52916E-03	0.79269E+06	0.36504E+08	0.59008E+08	0.50847E+08
0.40000E-02	0.12900	-0.53148E-03	0.98086E+06	0.24209E+08	0.46823E+08	0.39701E+08
0.45000E-02	0.12950	-0.53373E-03	0.11187E+07	0.12006E+08	0.34796E+08	0.29767E+08
0.50000E-02	0.13000	-0.53593E-03	0.12118E+07	-0.12029E+06	0.22903E+08	0.22387E+08
0.55000E-02	0.13050	-0.53807E-03	0.12612E+07	-0.12170E+08	0.11140E+08	0.20265E+08
0.60000E-02	0.13100	-0.54016E-03	0.12680E+07	-0.24145E+08	-0.49472E+06	0.24579E+08
0.65000E-02	0.13150	-0.54218E-03	0.12264E+07	-0.36035E+08	-0.11981E+08	0.32722E+08
0.70000E-02	0.13200	-0.54414E-03	0.11448E+07	-0.47851E+08	-0.23341E+08	0.42432E+08
0.75000E-02	0.13250	-0.54605E-03	0.10243E+07	-0.59597E+08	-0.34576E+08	0.52766E+08
0.80000E-02	0.13300	-0.54791E-03	0.86617E+06	-0.71273E+08	-0.45685E+08	0.63348E+08
0.85000E-02	0.13350	-0.54970E-03	0.66634E+06	-0.82869E+08	-0.56646E+08	0.73995E+08
0.90000E-02	0.13400	-0.55144E-03	0.43483E+06	-0.94398E+08	-0.67475E+08	0.84646E+08
0.95000E-02	0.13450	-0.55313E-03	0.16959E+06	-0.10588E+09	-0.78168E+08	0.95264E+08
0.10000E-01	0.13500	-0.55477E-03	-0.20577E+06	-0.11762E+09	-0.89034E+08	0.10605E+09

Table 7: Result comparison between theoretical and actual Von Mises stress at the entrance region.

Radial distance across thickness (m)	Von Mises Stress, S_EQV (Pa)		Ratio
	Theoretical	ANSYS	
0.125	0.13673e9	0.14307e9	1.046
0.1255	0.12413e9	0.12878e9	1.037
0.126	0.11170e9	0.11496e9	1.029
0.1265	0.99446e8	0.10139e9	1.019
0.127	0.87396e8	0.88093e8	1.008
0.1275	0.75581e8	0.75149e8	0.994
0.128	0.64056e8	0.62696e8	0.979
0.1285	0.52926e8	0.50847e8	0.961
0.129	0.42401e8	0.39701e8	0.936
0.1295	0.32934e8	0.29767e8	0.904
0.13	0.25560e8	0.22387e8	0.876
0.1305	0.22266e8	0.20265e8	0.910
0.131	0.24583e8	0.24579e8	1.000
0.1315	0.31168e8	0.32722e8	1.050
0.132	0.39873e8	0.42432e8	1.064
0.1325	0.49521e8	0.52766e8	1.066
0.133	0.59600e8	0.63348e8	1.063
0.1335	0.69875e8	0.73995e8	1.060
0.134	0.80230e8	0.84646e8	1.055
0.1345	0.90604e8	0.95264e8	1.051
0.135	0.10096e9	0.10605e9	1.050

As showed on the figure 13 below, hoop stress (SZ) and von Mises stress (SEQV) decrease linearly across the tube's thickness. While hoop stress continues decreasing linearly throughout the entire thickness, Von Mises stress starts to increase at a radial distance = 0.0055 meter from the inner surface. An important feature of this graph is that the peak stress occurs in the hoop direction which is equal to 151.83 MPa. Figure 14(a) below showed the contour plot of von mises stress distribution at the process entry side. Noted that the maximum von mises stress which is equal to 143.07 MPa occur at the inner surface of the process entry side.

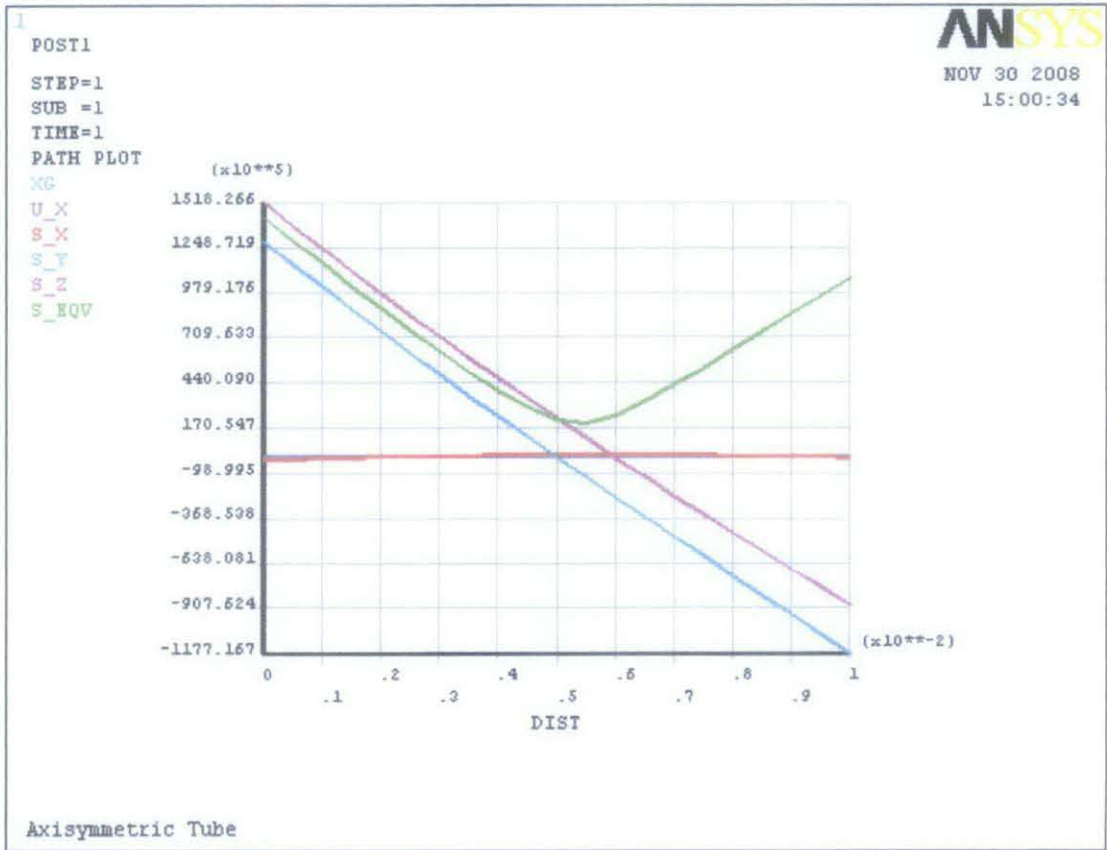
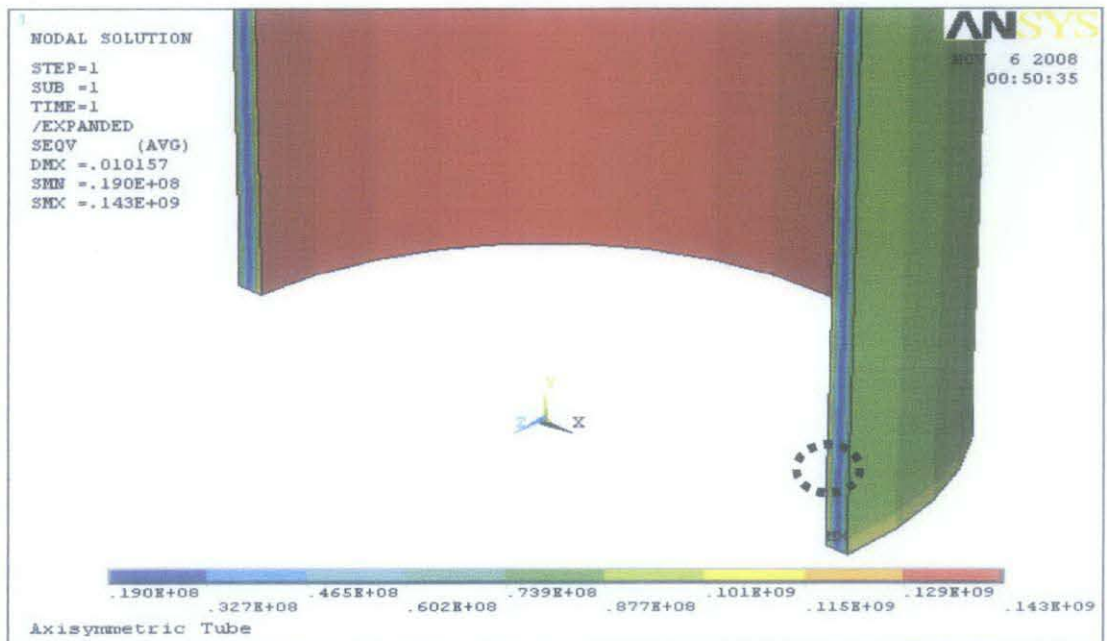
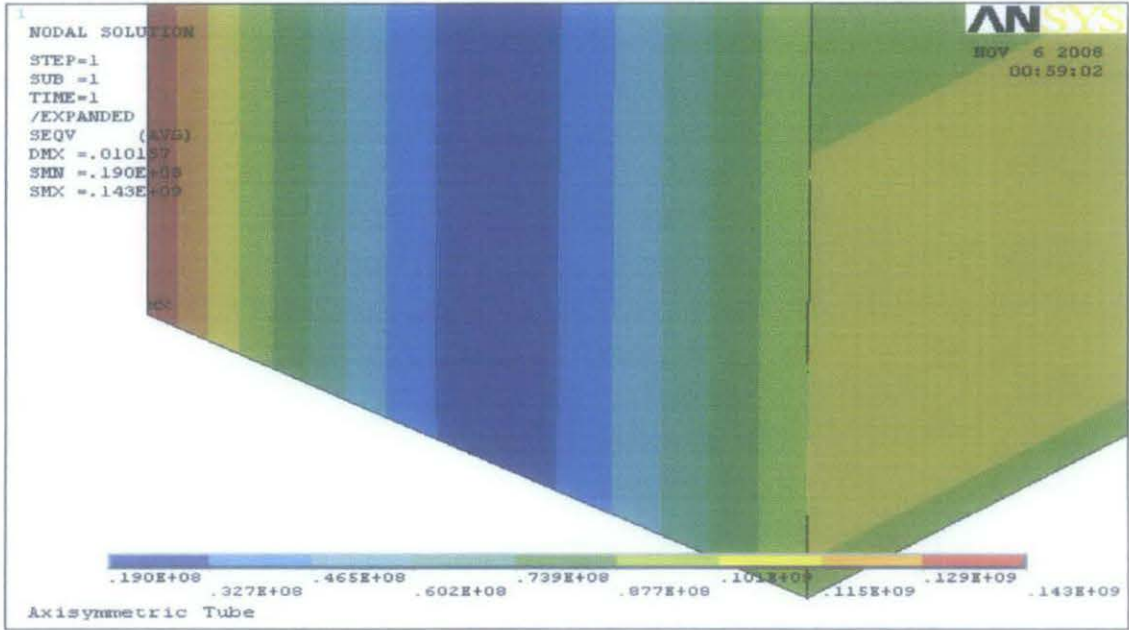


Figure 13 : Graph of stresses distribution at the entrance region



(a)



(b)

Figure 14: Contour plot of the stresses distribution at the entrance region showing maximum Von Mises stress.

2. At the middle length of the tube

Table 8: Stresses distribution across the tube's thickness at the middle of the length.

```

PRINT ALONG PATH DEFINED BY LPATH COMMAND.  DSYS= 0
***** PATH VARIABLE SUMMARY *****

```

S	XG	U_X	S_X	S_Y	S_Z	S_EQV
0.0000	0.12500	-0.21288E-04	0.20279E+07	0.57478E+08	0.84390E+08	0.76594E+08
0.50000E-03	0.12550	-0.21849E-04	0.16980E+07	0.51541E+08	0.78071E+08	0.70361E+08
0.10000E-02	0.12600	-0.22377E-04	0.13943E+07	0.45695E+08	0.71870E+08	0.64305E+08
0.15000E-02	0.12650	-0.22871E-04	0.11164E+07	0.39883E+08	0.65729E+08	0.58383E+08
0.20000E-02	0.12700	-0.23332E-04	0.86364E+06	0.34104E+08	0.59647E+08	0.52616E+08
0.25000E-02	0.12750	-0.23755E-04	0.63967E+06	0.28364E+08	0.53634E+08	0.47040E+08
0.30000E-02	0.12800	-0.24145E-04	0.43981E+06	0.22657E+08	0.47678E+08	0.41683E+08
0.35000E-02	0.12850	-0.24503E-04	0.26358E+06	0.16982E+08	0.41780E+08	0.36606E+08
0.40000E-02	0.12900	-0.24828E-04	0.11054E+06	0.11340E+08	0.35937E+08	0.31903E+08
0.45000E-02	0.12950	-0.25115E-04	16072.	0.57356E+07	0.30159E+08	0.27729E+08
0.50000E-02	0.13000	-0.25371E-04	0.12053E+06	0.16296E+06	0.24435E+08	0.24293E+08
0.55000E-02	0.13050	-0.25595E-04	0.20325E+06	-0.53781E+07	0.18765E+08	0.21892E+08
0.60000E-02	0.13100	-0.25788E-04	0.26468E+06	-0.10888E+08	0.13148E+08	0.20833E+08
0.65000E-02	0.13150	-0.25943E-04	0.30180E+06	-0.16361E+08	0.75914E+07	0.21266E+08
0.70000E-02	0.13200	-0.26068E-04	0.31855E+06	-0.21803E+08	0.20867E+07	0.23057E+08
0.75000E-02	0.13250	-0.26162E-04	0.31533E+06	-0.27215E+08	-0.33672E+07	0.25886E+08
0.80000E-02	0.13300	-0.26225E-04	0.29252E+06	-0.32596E+08	-0.87709E+07	0.29423E+08
0.85000E-02	0.13350	-0.26252E-04	0.24736E+06	-0.37942E+08	-0.14117E+08	0.33410E+08
0.90000E-02	0.13400	-0.26249E-04	0.18348E+06	-0.43258E+08	-0.19414E+08	0.37682E+08
0.95000E-02	0.13450	-0.26215E-04	0.10124E+06	-0.48545E+08	-0.24663E+08	0.42131E+08
0.10000E-01	0.13500	-0.26151E-04	987.99	-0.53806E+08	-0.29869E+08	0.46692E+08

Table 9: Result comparison between theoretical and actual Von Mises stress at the middle of the tube's length.

Radial distance across thickness (m)	Von Mises Stress, S_EQV (Pa)		Ratio
	Theoretical	ANSYS	
0.125	0.71911e8	0.76594e8	1.065
0.1255	0.66323e8	0.70361e8	1.061
0.126	0.60842e8	0.64305e8	1.057
0.1265	0.55482e8	0.58383e8	1.052
0.127	0.50260e8	0.52616e8	1.047
0.1275	0.45201e8	0.47040e8	1.041
0.128	0.40342e8	0.41683e8	1.034
0.1285	0.35737e8	0.36606e8	1.024
0.129	0.31471e8	0.31903e8	1.014
0.1295	0.27665e8	0.27729e8	1.002
0.13	0.24500e8	0.24293e8	0.992
0.1305	0.22213e8	0.21892e8	0.986
0.131	0.21053e8	0.20833e8	0.990
0.1315	0.21167e8	0.21266e8	1.005
0.132	0.22501e8	0.23057e8	1.025
0.1325	0.24830e8	0.25886e8	1.043
0.133	0.27880e8	0.29423e8	1.055
0.1335	0.31418e8	0.33410e8	1.063
0.134	0.35279e8	0.37682e8	1.068
0.1345	0.39351e8	0.42131e8	1.071
0.135	0.43560e8	0.46692e8	1.072

The pattern of stresses distribution across the tube's thickness in middle of the tube's length is the same as the previous one, which is at the process entry side. As shown on Figure 15 below, hoop stress (SZ) and von Mises stress (SEQV) also decrease linearly across the tube's thickness. While hoop stress continues decreasing linearly throughout the entire thickness, Von Mises stress starts to increase at a radial distance = 0.006 meter from the inner surface. It is also showed that there are only little increases for

displacement UX and radial stress (SX). The peak stress at the middle of the tube is also the hoop stress which is equal to 84.39 MPa. Note that the value of the peak stress is lower compared to the peak stress at the process entry side.

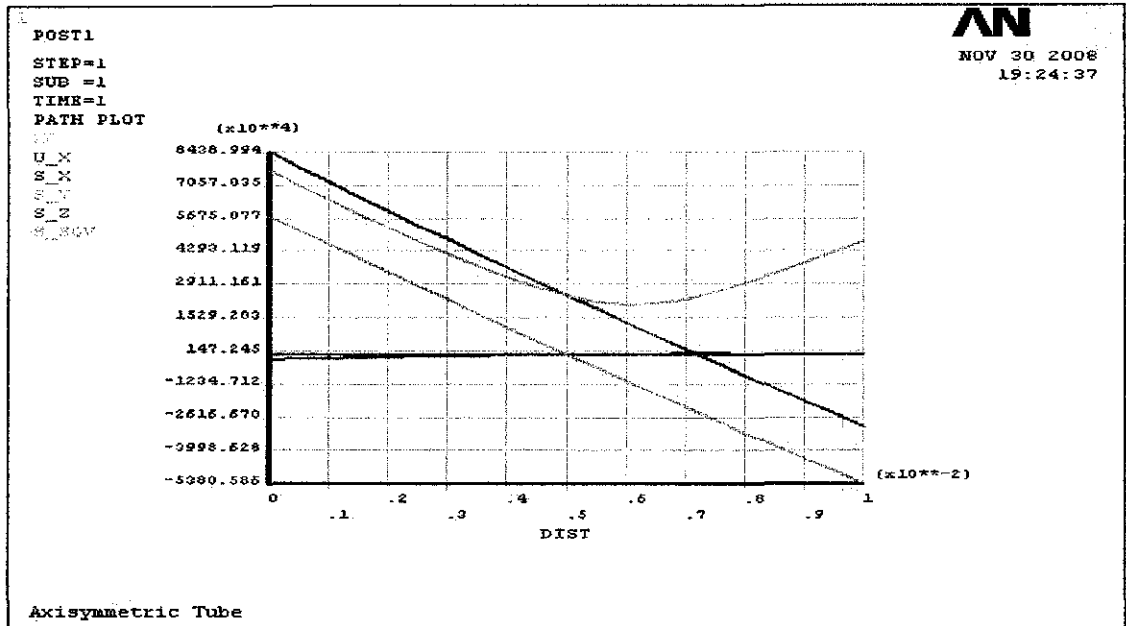


Figure 15: Graph of stresses distribution at the middle length of the tube.

3. At process exit side

Table 10: Stress distribution across the tube's thickness at the exit region.

```
PRINT ALONG PATH DEFINED BY LPATH COMMAND. DSYS= 0
***** PATH VARIABLE SUMMARY *****
```

S	XG	U_X	S_X	S_Y	S_Z	S_EQV
0.0000	0.12500	0.36605E-04	-0.22387E+07	0.14029E+08	0.43320E+08	0.39989E+08
0.50000E-03	0.12550	0.36485E-04	-0.20603E+07	0.12605E+08	0.41703E+08	0.38581E+08
0.10000E-02	0.12600	0.36374E-04	-0.18899E+07	0.11188E+08	0.40100E+08	0.37217E+08
0.15000E-02	0.12650	0.36272E-04	-0.17270E+07	0.97768E+07	0.38511E+08	0.35897E+08
0.20000E-02	0.12700	0.36180E-04	-0.15713E+07	0.83717E+07	0.36936E+08	0.34624E+08
0.25000E-02	0.12750	0.36097E-04	-0.14239E+07	0.69737E+07	0.35376E+08	0.33403E+08
0.30000E-02	0.12800	0.36024E-04	-0.12834E+07	0.55817E+07	0.33830E+08	0.32234E+08
0.35000E-02	0.12850	0.35959E-04	-0.11497E+07	0.41957E+07	0.32296E+08	0.31119E+08
0.40000E-02	0.12900	0.35902E-04	-0.10227E+07	0.28156E+07	0.30775E+08	0.30063E+08
0.45000E-02	0.12950	0.35856E-04	-0.90328E+06	0.14424E+07	0.29268E+08	0.29070E+08
0.50000E-02	0.13000	0.35819E-04	-0.79032E+06	74931.	0.27774E+08	0.28142E+08
0.55000E-02	0.13050	0.35790E-04	-0.68367E+06	-0.12867E+07	0.26292E+08	0.27283E+08
0.60000E-02	0.13100	0.35769E-04	-0.58321E+06	-0.26427E+07	0.24822E+08	0.26496E+08
0.65000E-02	0.13150	0.35758E-04	-0.48983E+06	-0.39920E+07	0.23366E+08	0.25786E+08
0.70000E-02	0.13200	0.35755E-04	-0.40240E+06	-0.53357E+07	0.21922E+08	0.25157E+08
0.75000E-02	0.13250	0.35761E-04	-0.32082E+06	-0.66738E+07	0.20489E+08	0.24610E+08
0.80000E-02	0.13300	0.35774E-04	-0.24497E+06	-0.80064E+07	0.19068E+08	0.24148E+08
0.85000E-02	0.13350	0.35798E-04	-0.17569E+06	-0.93326E+07	0.17660E+08	0.23775E+08
0.90000E-02	0.13400	0.35829E-04	-0.11191E+06	-0.10653E+08	0.16263E+08	0.23492E+08
0.95000E-02	0.13450	0.35868E-04	-53467.	-0.11969E+08	0.14876E+08	0.23297E+08
0.10000E-01	0.13500	0.35915E-04	-1238.1	-0.13278E+08	0.13502E+08	0.23192E+08

Table 11: Result comparison between theoretical and actual Von Mises stress at the exit region.

Radial distance across thickness (m)	Von Mises Stress, S_EQV (Pa)		Ratio
	Theoretical	ANSYS	
0.125	0.33808e8	0.39989e8	1.183
0.1255	0.32497e8	0.38581e8	1.187
0.126	0.31227e8	0.37217e8	1.192
0.1265	0.29999e8	0.35897e8	1.197
0.127	0.28816e8	0.34624e8	1.201
0.1275	0.27680e8	0.33403e8	1.207
0.128	0.26595e8	0.32234e8	1.212
0.1285	0.25564e8	0.31119e8	1.217
0.129	0.24591e8	0.30063e8	1.223
0.1295	0.23681e8	0.29070e8	1.228
0.13	0.22838e8	0.28142e8	1.232
0.1305	0.22067e8	0.27283e8	1.236
0.131	0.21372e8	0.26496e8	1.240
0.1315	0.20758e8	0.25786e8	1.242
0.132	0.20230e8	0.25157e8	1.244
0.1325	0.19791e8	0.24610e8	1.243
0.133	0.19445e8	0.24148e8	1.242
0.1335	0.19194e8	0.23775e8	1.239
0.134	0.19038e8	0.23492e8	1.234
0.1345	0.18978e8	0.23297e8	1.228
0.135	0.19011e8	0.23192e8	1.220

Figure 16 below showed that, at the process exit side, the hoop stress (SZ) and the von mises stress (SEQV) decreases across the tube's thickness. There is only a slight increase in the radial stress (SX). The peak value of hoop stress which is equal to 43.32 MPa at the inner surface decreases to 13.5 MPa at the outer surface of the tube. Figure 17 shows the von mises stress distribution at the process exit side. It can be seen that the inner surface experiencing higher stress compared to the outer surface which is experiencing minimum von mises stress.

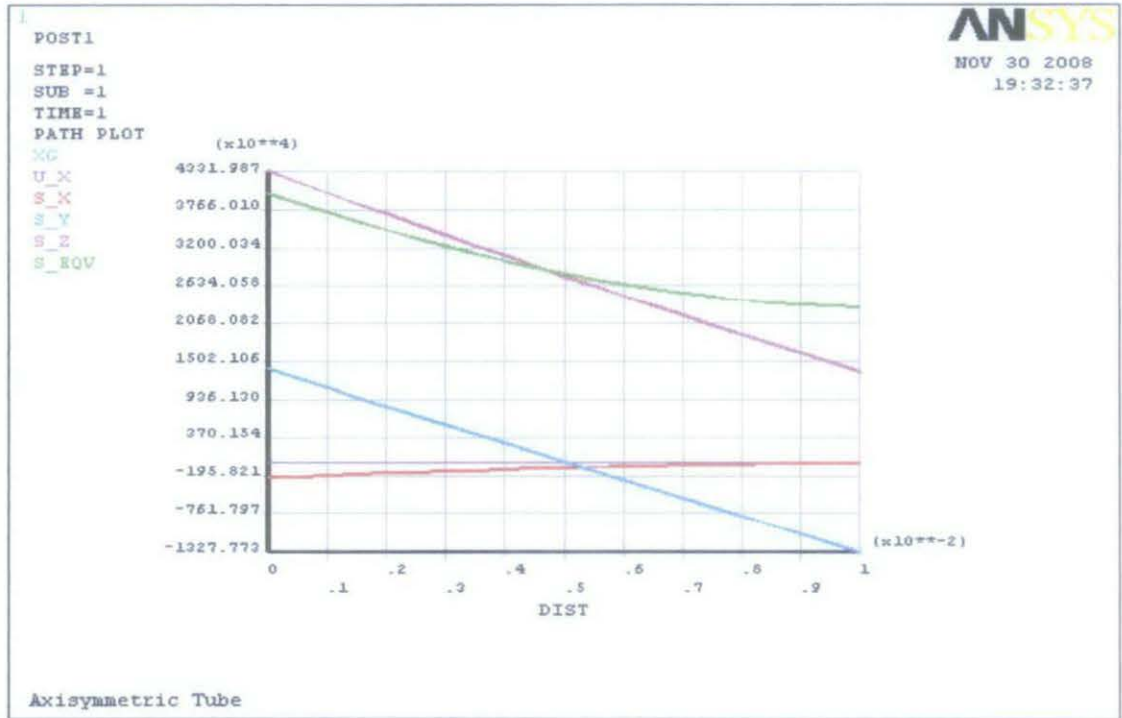


Figure 16: Graph of stress distribution at the tube's process exit

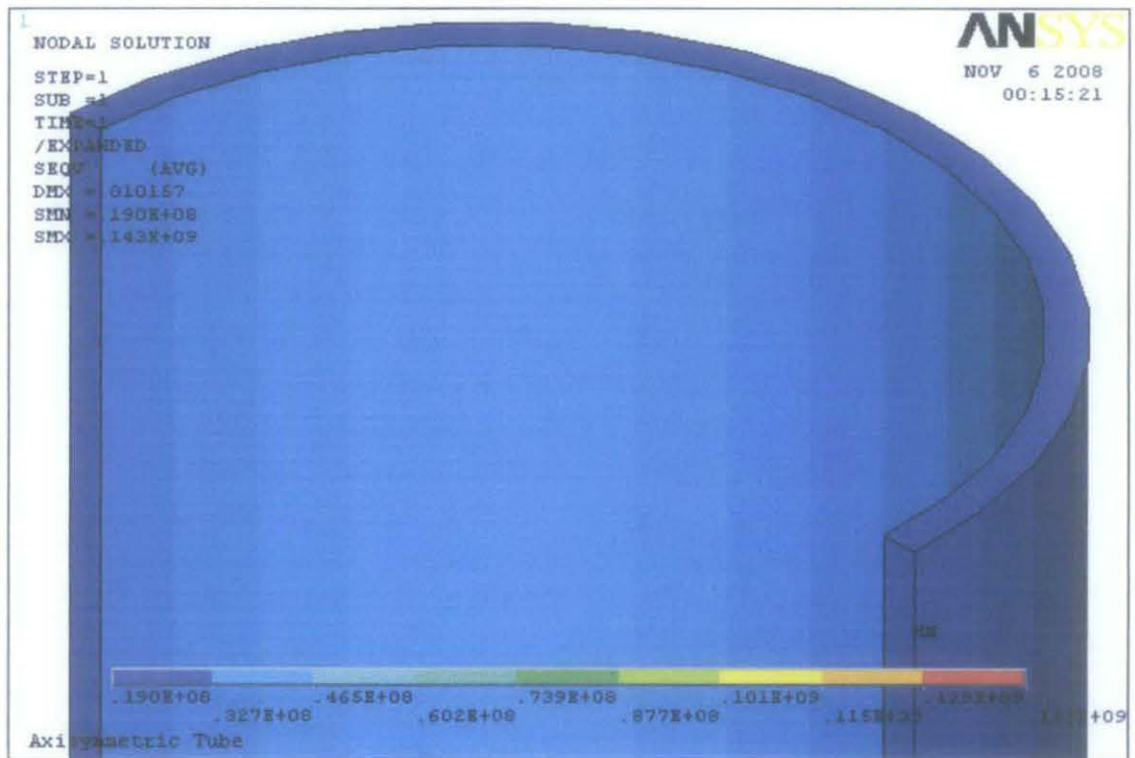


Figure 17: Contour plot of Von Mises stress distribution at the exit region.

4.4.2 Stress distribution across the tube's length

1. At the inner surface

Table 12: Stress distribution on the inner surface across the tube's length.

S	XG	U_X	S_X	S_Y	S_Z	S_EQV
0.0000	0.12500	-0.51121E-03	-0.17180E+07	0.12793E+09	0.15178E+09	0.14307E+09
0.20000	0.12500	-0.46786E-03	-0.18235E+07	0.11572E+09	0.13999E+09	0.13137E+09
0.40000	0.12500	-0.42055E-03	-0.18302E+07	0.11160E+09	0.13595E+09	0.12737E+09
0.60000	0.12500	-0.37321E-03	-0.18370E+07	0.10730E+09	0.13184E+09	0.12325E+09
0.80000	0.12500	-0.33088E-03	-0.18437E+07	0.10566E+09	0.13019E+09	0.12164E+09
1.0000	0.12500	-0.28828E-03	-0.18504E+07	0.10371E+09	0.12832E+09	0.11977E+09
1.2000	0.12500	-0.24711E-03	-0.18572E+07	0.10143E+09	0.12653E+09	0.11786E+09
1.4000	0.12500	-0.21902E-03	-0.18638E+07	0.10229E+09	0.12708E+09	0.11851E+09
1.6000	0.12500	-0.19082E-03	-0.18705E+07	0.10247E+09	0.12737E+09	0.11877E+09
1.8000	0.12500	-0.16460E-03	-0.18771E+07	0.10236E+09	0.12764E+09	0.11891E+09
2.0000	0.12500	-0.14840E-03	-0.18837E+07	0.10345E+09	0.12858E+09	0.11989E+09
2.2000	0.12500	-0.13209E-03	-0.18904E+07	0.10424E+09	0.12949E+09	0.12075E+09
2.4000	0.12500	-0.11686E-03	-0.18970E+07	0.10474E+09	0.13019E+09	0.12138E+09
2.6000	0.12500	-0.10553E-03	-0.19037E+07	0.10455E+09	0.13004E+09	0.12123E+09
2.8000	0.12500	-0.94124E-04	-0.19103E+07	0.10473E+09	0.12994E+09	0.12110E+09
3.0000	0.12500	-0.83451E-04	-0.19170E+07	0.10365E+09	0.12939E+09	0.12051E+09
3.2000	0.12500	-0.74680E-04	-0.19237E+07	0.10182E+09	0.12766E+09	0.11879E+09
3.4000	0.12500	-0.65865E-04	-0.19304E+07	0.10014E+09	0.12608E+09	0.11721E+09
3.6000	0.12500	-0.58099E-04	-0.19371E+07	0.98036E+08	0.12406E+09	0.11521E+09
3.8000	0.12500	-0.52325E-04	-0.19438E+07	0.95147E+08	0.12123E+09	0.11243E+09
4.0000	0.12500	-0.46614E-04	-0.19516E+07	0.92100E+08	0.11829E+09	0.10952E+09
4.2000	0.12500	-0.43223E-04	-0.19573E+07	0.88988E+08	0.11521E+09	0.10651E+09
4.4000	0.12500	-0.40117E-04	-0.19640E+07	0.85712E+08	0.11200E+09	0.10336E+09
4.6000	0.12500	-0.36897E-04	-0.19708E+07	0.82417E+08	0.10879E+09	0.10021E+09
4.8000	0.12500	-0.34768E-04	-0.19775E+07	0.79237E+08	0.10565E+09	0.97155E+08
5.0000	0.12500	-0.32905E-04	-0.19842E+07	0.76056E+08	0.10254E+09	0.94118E+08
5.2000	0.12500	-0.31041E-04	-0.19910E+07	0.72877E+08	0.99424E+08	0.91091E+08
5.4000	0.12500	-0.29299E-04	-0.19977E+07	0.69863E+08	0.96476E+08	0.88230E+08
5.6000	0.12500	-0.27639E-04	-0.20044E+07	0.66962E+08	0.93640E+08	0.85487E+08
5.8000	0.12500	-0.25978E-04	-0.20111E+07	0.64063E+08	0.90807E+08	0.82751E+08
6.0000	0.12500	-0.24277E-04	-0.20179E+07	0.61251E+08	0.88059E+08	0.80111E+08
6.2000	0.12500	-0.22306E-04	-0.20246E+07	0.58719E+08	0.85597E+08	0.77749E+08
6.4000	0.12500	-0.20270E-04	-0.20313E+07	0.56237E+08	0.83183E+08	0.75441E+08
6.6000	0.12500	-0.18234E-04	-0.20380E+07	0.53755E+08	0.80770E+08	0.73143E+08
6.8000	0.12500	-0.16053E-04	-0.20447E+07	0.51512E+08	0.78596E+08	0.71080E+08
7.0000	0.12500	-0.13793E-04	-0.20514E+07	0.49397E+08	0.76552E+08	0.69148E+08
7.2000	0.12500	-0.11532E-04	-0.20581E+07	0.47283E+08	0.74509E+08	0.67224E+08
7.4000	0.12500	-0.90948E-05	-0.20648E+07	0.45297E+08	0.72595E+08	0.65431E+08
7.6000	0.12500	-0.65116E-05	-0.20715E+07	0.43418E+08	0.70788E+08	0.63745E+08
7.8000	0.12500	-0.39257E-05	-0.20782E+07	0.41540E+08	0.68981E+08	0.62069E+08
8.0000	0.12500	-0.12888E-05	-0.20849E+07	0.39803E+08	0.67318E+08	0.60533E+08
8.2000	0.12500	0.14129E-05	-0.20916E+07	0.38247E+08	0.65836E+08	0.59171E+08
8.4000	0.12500	0.41176E-05	-0.20983E+07	0.36691E+08	0.64354E+08	0.57818E+08
8.6000	0.12500	0.68727E-05	-0.21050E+07	0.35196E+08	0.62934E+08	0.56528E+08
8.8000	0.12500	0.97287E-05	-0.21117E+07	0.33825E+08	0.61639E+08	0.55358E+08
9.0000	0.12500	0.12587E-04	-0.21184E+07	0.32453E+08	0.60343E+08	0.54196E+08
9.2000	0.12500	0.15450E-04	-0.21251E+07	0.31103E+08	0.59068E+08	0.53060E+08
9.4000	0.12500	0.18320E-04	-0.21318E+07	0.29822E+08	0.57864E+08	0.51994E+08
9.6000	0.12500	0.21194E-04	-0.21384E+07	0.28542E+08	0.56659E+08	0.50936E+08
9.8000	0.12500	0.23726E-04	-0.21451E+07	0.27100E+08	0.55365E+08	0.49807E+08
10.000	0.12500	0.23826E-04	-0.21518E+07	0.25311E+08	0.53573E+08	0.48261E+08
10.200	0.12500	0.23941E-04	-0.21585E+07	0.23436E+08	0.51770E+08	0.46724E+08
10.400	0.12500	0.23979E-04	-0.21652E+07	0.21755E+08	0.50159E+08	0.45370E+08
10.600	0.12500	0.23975E-04	-0.21719E+07	0.20178E+08	0.48655E+08	0.44124E+08
10.800	0.12500	0.23955E-04	-0.21786E+07	0.18619E+08	0.47142E+08	0.42887E+08
11.000	0.12500	0.23929E-04	-0.21853E+07	0.17604E+08	0.46231E+08	0.42162E+08
11.200	0.12500	0.26977E-04	-0.21919E+07	0.16764E+08	0.45470E+08	0.41563E+08
11.400	0.12500	0.28664E-04	-0.21986E+07	0.15954E+08	0.44719E+08	0.40977E+08
11.600	0.12500	0.30896E-04	-0.22053E+07	0.15315E+08	0.44181E+08	0.40571E+08
11.800	0.12500	0.33171E-04	-0.22120E+07	0.14723E+08	0.43671E+08	0.40187E+08
12.000	0.12500	0.35442E-04	-0.22186E+07	0.14161E+08	0.43182E+08	0.39823E+08
12.200	0.12500	0.36581E-04	-0.22253E+07	0.14035E+08	0.43149E+08	0.39817E+08
12.400	0.12500	0.36593E-04	-0.22319E+07	0.14031E+08	0.43234E+08	0.39902E+08
12.600	0.12500	0.36605E-04	-0.22387E+07	0.14029E+08	0.43320E+08	0.39989E+08

Table 13: Result comparison between theoretical and actual Von Mises stress on the inner surface.

Distance down the tube length (m)	Von Mises		Ratio
	Theoretical	ANSYS	
0.00	0.13671e9	0.14307e9	1.047
0.60	0.12600e9	0.12325e9	0.978
1.20	0.12135e9	0.11786e9	0.971
1.80	0.12274e9	0.11891e9	0.969
2.60	0.12587e9	0.12123e9	0.963
3.20	0.11368e9	0.11879e9	1.045
3.80	0.10300e9	0.11243e9	1.092
4.40	0.92659e8	0.10336e9	1.115
5.00	0.83226e8	0.94118e8	1.131
5.60	0.81489e8	0.85487e8	1.049
6.60	0.73689e8	0.73143e8	0.993
7.00	0.67066e8	0.69148e8	1.031
7.60	0.61194e8	0.63745e8	1.042
8.20	0.56335e8	0.59171e8	1.050
8.80	0.52067e8	0.55358e8	1.063
9.40	0.48118e8	0.51994e8	1.081
10.00	0.43637e8	0.48261e8	1.106
10.80	0.39368e8	0.42887e8	1.089
11.40	0.37047e8	0.40977e8	1.106
12.00	0.35365e8	0.39823e8	1.126
12.60	0.35011e8	0.39989e8	1.142

Figure 18 shows the steady state stress with the inner surface for the reformer tube along the length of computational region. As can be seen from this figure, the hoop stress values increase to the value of about $y=1.26$ m, then it slightly rise and decline steadily after $y=3.15$ m. The other stresses which are radial (SX) and axial (SY) stresses behaves in the same pattern as the hoop stress, only with lower value of stresses.

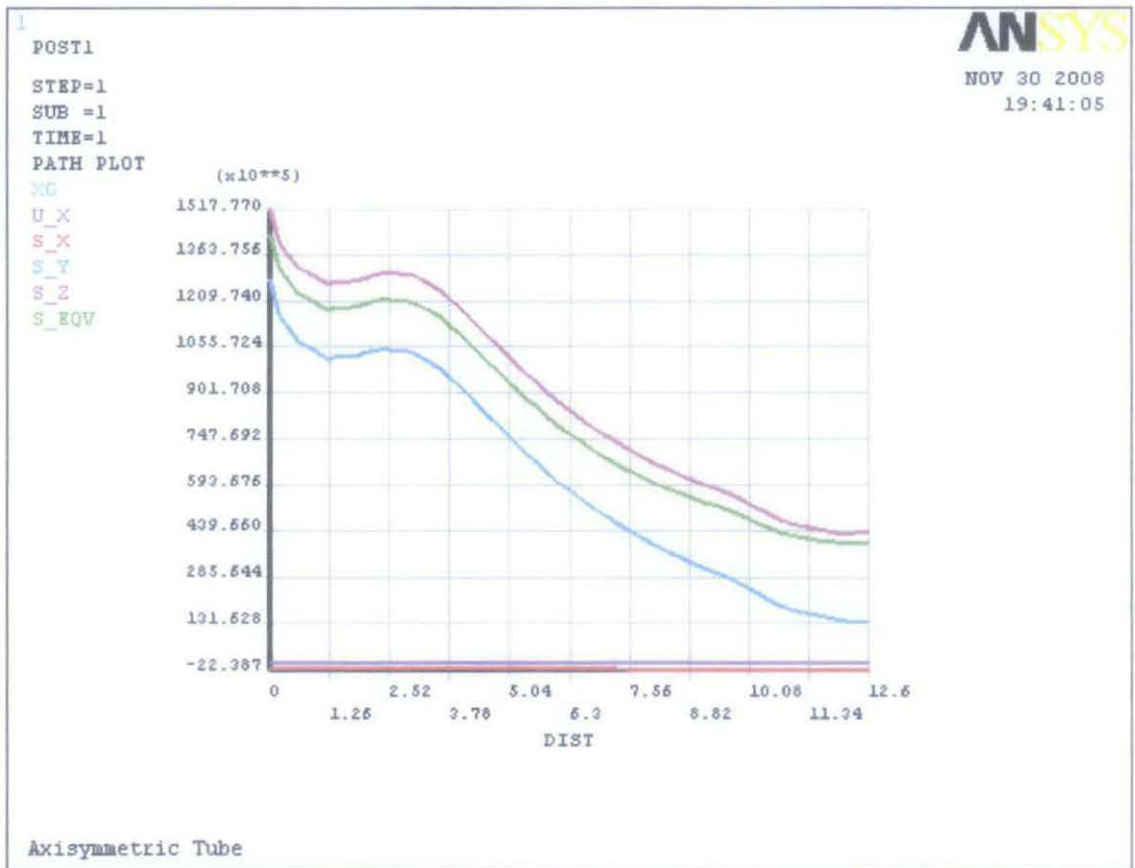


Figure 18: Stress distribution on the inner surface across the tube's length.

2. At the outer surface

Table 14: Stress distribution on the outer surface across the tube's length.

S	XG	U_X	S_X	S_Y	S_Z	S_EQV
0.0000	0.13500	-0.55477E-03	-0.20577E+06	-0.11762E+09	-0.89034E+08	0.10605E+09
0.20000	0.13500	-0.50768E-03	2049.7	-0.10782E+09	-0.86328E+08	0.98845E+08
0.40000	0.13500	-0.45664E-03	1965.0	-0.10400E+09	-0.82415E+08	0.95062E+08
0.60000	0.13500	-0.40554E-03	1853.5	-0.99992E+08	-0.78631E+08	0.91209E+08
0.80000	0.13500	-0.35989E-03	1832.3	-0.98457E+08	-0.76715E+08	0.89589E+08
1.0000	0.13500	-0.31392E-03	1787.5	-0.96619E+08	-0.74799E+08	0.87769E+08
1.2000	0.13500	-0.26950E-03	1735.1	-0.94479E+08	-0.72968E+08	0.85773E+08
1.4000	0.13500	-0.23919E-03	1736.3	-0.95239E+08	-0.73269E+08	0.86377E+08
1.6000	0.13500	-0.20877E-03	1745.9	-0.94760E+08	-0.72782E+08	0.85908E+08
1.8000	0.13500	-0.18048E-03	1742.6	-0.94322E+08	-0.72449E+08	0.85512E+08
2.0000	0.13500	-0.16300E-03	1739.2	-0.95269E+08	-0.73229E+08	0.86386E+08
2.2000	0.13500	-0.14540E-03	1747.7	-0.96037E+08	-0.73952E+08	0.87121E+08
2.4000	0.13500	-0.12897E-03	1755.3	-0.96596E+08	-0.74454E+08	0.87650E+08
2.6000	0.13500	-0.11675E-03	1741.3	-0.96534E+08	-0.74329E+08	0.87571E+08
2.8000	0.13500	-0.10445E-03	1734.7	-0.96449E+08	-0.74178E+08	0.87469E+08
3.0000	0.13500	-0.92949E-04	1721.6	-0.95941E+08	-0.73582E+08	0.86947E+08
3.2000	0.13500	-0.83499E-04	1688.4	-0.94389E+08	-0.71961E+08	0.85414E+08
3.4000	0.13500	-0.74003E-04	1658.5	-0.92847E+08	-0.70334E+08	0.83889E+08
3.6000	0.13500	-0.65641E-04	1622.1	-0.90925E+08	-0.68310E+08	0.81993E+08
3.8000	0.13500	-0.59428E-04	1574.0	-0.88295E+08	-0.65598E+08	0.79419E+08
4.0000	0.13500	-0.53277E-04	166.91	-0.85517E+08	-0.62902E+08	0.76751E+08
4.2000	0.13500	-0.49752E-04	1475.6	-0.82685E+08	-0.59793E+08	0.73948E+08
4.4000	0.13500	-0.46310E-04	1425.2	-0.79700E+08	-0.56708E+08	0.71053E+08
4.6000	0.13500	-0.42856E-04	1376.4	-0.76693E+08	-0.53607E+08	0.68150E+08
4.8000	0.13500	-0.40575E-04	1324.6	-0.73789E+08	-0.50597E+08	0.65357E+08
5.0000	0.13500	-0.38582E-04	1275.9	-0.70880E+08	-0.47587E+08	0.62575E+08
5.2000	0.13500	-0.36588E-04	1227.2	-0.67969E+08	-0.44575E+08	0.59809E+08
5.4000	0.13500	-0.34725E-04	1180.5	-0.65205E+08	-0.41712E+08	0.57201E+08
5.6000	0.13500	-0.32950E-04	1135.6	-0.62541E+08	-0.38949E+08	0.54705E+08
5.8000	0.13500	-0.31173E-04	1090.7	-0.59875E+08	-0.36183E+08	0.52229E+08
6.0000	0.13500	-0.29354E-04	1046.5	-0.57286E+08	-0.33497E+08	0.49849E+08
6.2000	0.13500	-0.27242E-04	1007.5	-0.54951E+08	-0.31063E+08	0.47725E+08
6.4000	0.13500	-0.25060E-04	968.47	-0.52660E+08	-0.28675E+08	0.45666E+08
6.6000	0.13500	-0.22878E-04	929.23	-0.50366E+08	-0.26285E+08	0.43633E+08
6.8000	0.13500	-0.20539E-04	894.08	-0.48290E+08	-0.24112E+08	0.41821E+08
7.0000	0.13500	-0.18114E-04	860.47	-0.46332E+08	-0.22059E+08	0.40140E+08
7.2000	0.13500	-0.15688E-04	826.81	-0.44371E+08	-0.20005E+08	0.38489E+08
7.4000	0.13500	-0.13073E-04	795.37	-0.42528E+08	-0.18067E+08	0.36970E+08
7.6000	0.13500	-0.10300E-04	765.25	-0.40783E+08	-0.16228E+08	0.35564E+08
7.8000	0.13500	-0.75231E-05	735.16	-0.39036E+08	-0.14388E+08	0.34194E+08
8.0000	0.13500	-0.46914E-05	707.36	-0.37419E+08	-0.12679E+08	0.32963E+08
8.2000	0.13500	-0.17895E-05	682.25	-0.35970E+08	-0.11138E+08	0.31895E+08
8.4000	0.13500	0.11155E-05	657.17	-0.34520E+08	-0.95966E+07	0.30862E+08
8.6000	0.13500	0.40752E-05	632.99	-0.33126E+08	-0.81124E+07	0.29907E+08
8.8000	0.13500	0.71437E-05	610.91	-0.31846E+08	-0.67413E+07	0.29068E+08
9.0000	0.13500	0.10215E-04	588.70	-0.30565E+08	-0.53702E+07	0.28265E+08
9.2000	0.13500	0.13290E-04	566.76	-0.29302E+08	-0.40184E+07	0.27514E+08
9.4000	0.13500	0.16375E-04	546.07	-0.28105E+08	-0.27307E+07	0.26844E+08
9.6000	0.13500	0.19463E-04	525.26	-0.26906E+08	-0.14431E+07	0.26215E+08
9.8000	0.13500	0.22180E-04	504.81	-0.25555E+08	-46573.	0.25532E+08
10.000	0.13500	0.22278E-04	472.53	-0.23881E+08	0.17690E+07	0.24813E+08
10.200	0.13500	0.22390E-04	442.60	-0.22123E+08	0.36216E+07	0.24139E+08
10.400	0.13500	0.22419E-04	415.53	-0.20546E+08	0.52935E+07	0.23641E+08
10.600	0.13500	0.22403E-04	390.15	-0.19064E+08	0.68678E+07	0.23271E+08
10.800	0.13500	0.22372E-04	361.78	-0.17599E+08	0.84255E+07	0.23000E+08
11.000	0.13500	0.23801E-04	349.00	-0.16644E+08	0.94705E+07	0.22898E+08
11.200	0.13500	0.25607E-04	335.28	-0.15853E+08	0.10348E+08	0.22857E+08
11.400	0.13500	0.27415E-04	321.88	-0.15090E+08	0.11217E+08	0.22865E+08
11.600	0.13500	0.29811E-04	311.82	-0.14488E+08	0.11884E+08	0.22876E+08
11.800	0.13500	0.32254E-04	302.16	-0.13930E+08	0.12527E+08	0.22923E+08
12.000	0.13500	0.34693E-04	292.03	-0.13401E+08	0.13141E+08	0.22986E+08
12.200	0.13500	0.35911E-04	291.13	-0.13282E+08	0.13344E+08	0.23059E+08
12.400	0.13500	0.35912E-04	291.02	-0.13278E+08	0.13424E+08	0.23125E+08
12.600	0.13500	0.35915E-04	-1238.1	-0.13278E+08	0.13502E+08	0.23192E+08

Table 15: Result comparison between theoretical and actual Von Mises stress on the outer surface.

Distance down the tube length (m)	Von Mises Stress, S_EQV (Pa)		Ratio
	Theoretical	ANSYS	
0.00	0.10097e9	0.10605e9	1.050
0.60	0.91143e8	0.91209e8	1.001
1.20	0.87023e8	0.85773e8	0.986
1.80	0.88566e8	0.85512e8	0.966
2.60	0.87267e8	0.87571e8	1.003
3.20	0.80981e8	0.85414e8	1.055
3.80	0.71277e8	0.79419e8	1.114
4.40	0.61950e8	0.71053e8	1.147
5.00	0.53559e8	0.62575e8	1.168
5.60	0.52020e8	0.54705e8	1.052
6.60	0.45259e8	0.43633e8	0.964
7.00	0.39672e8	0.40140e8	1.012
7.60	0.34896e8	0.35564e8	1.019
8.20	0.31138e8	0.31895e8	1.024
8.80	0.28030e8	0.29068e8	1.037
9.40	0.25370e8	0.26844e8	1.058
10.00	0.22701e8	0.24813e8	1.093
10.80	0.20707e8	0.23000e8	1.111
11.40	0.19878e8	0.22865e8	1.150
12.00	0.19380e8	0.22986e8	1.186
12.60	0.19172e8	0.18985e8	0.990

Figure 19 shows the steady state stress with the outer surface for the reformer tube along the length of computational region. As can be seen from this figure, the hoop stress values increase to the value of about $y=1.26$ m in a compressive manner, then it is slightly declined and rise steadily after $y=3.15$ m. It is showed that the von mises stress distribution behaves with the opposite pattern of the hoop stress.

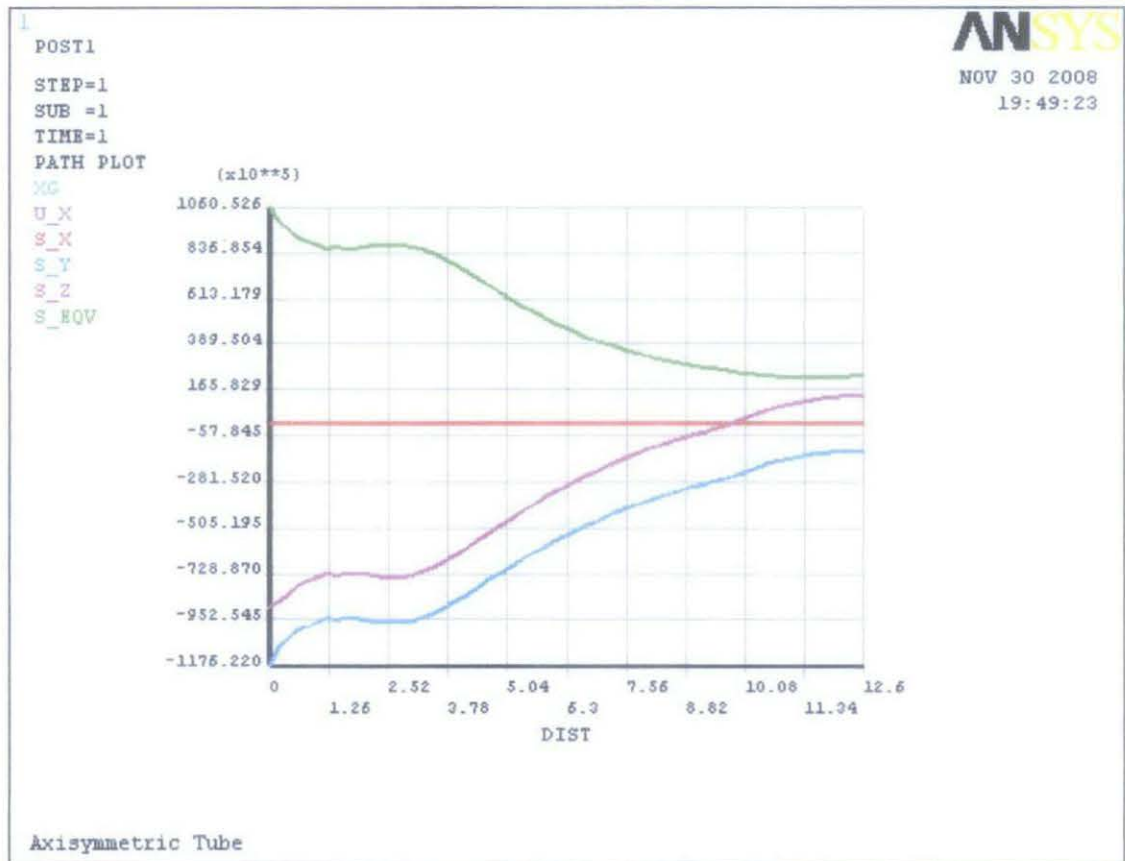


Figure 19: Stress distribution on the outer surface across the tube's length.

In the thermally developed flow of a fluid with constant properties, the heat transfer coefficient, h , is constant, independent of axial locations, x . Because of thermal boundary layer thickness is smaller at the tube entrance; the convection coefficient is extremely large at the pipe inlet region. However, the coefficient decays rapidly as the thermal boundary layer develops, until the constant value associated with fully developed conditions is reached. It is known that the temperature difference across the tube length resulted from the non-uniform heat transfer coefficient can be considerable causing of high thermal stresses [19].

4.5 Comparison with yield strength of the material

The maximum von mises stress obtained then compared with the tensile strength of the tube to determine whether the tube is able to sustain the load. Table 16 below shows the yield strength of the tube.

Table 16: Yield strength of the reformer tube.

Temperature (K)	773	873	973	1073	1173
Yield Strength (MPa)	260	232	200	160	112

The maximum von mises stress produced by the reformer tube is 143.07 MPa. The maximum von mises stress occurred at the inner surface of the entrance region which operates at temperature of 849.2 K.

As can be seen from table 16 above, since yield strength of the tube is 242.86 MPa for temperature equal to 849.2 K, thus the material is able to sustain the maximum von mises stress without fracture.

Table 17: Comparison of max. Von Mises stress with yield strength of the tube

Paths	Temperature at which max Von Mises stress occur (K)	Max Von Mises stress, $\sigma_{vm\ max}$ (MPa)	Yield strength at that temperature, σ_y (MPa)	Ratio $\sigma_{vm\ max} / \sigma_y$
Entrance	849.2	143.07	242.86	0.588
Middle	1108	76.59	142.86	0.536
Exit	1149	39.99	121.43	0.329
Inner Surface	849.2	143.07	242.86	0.588
Outer Surface	929.2	106.05	214.29	0.495

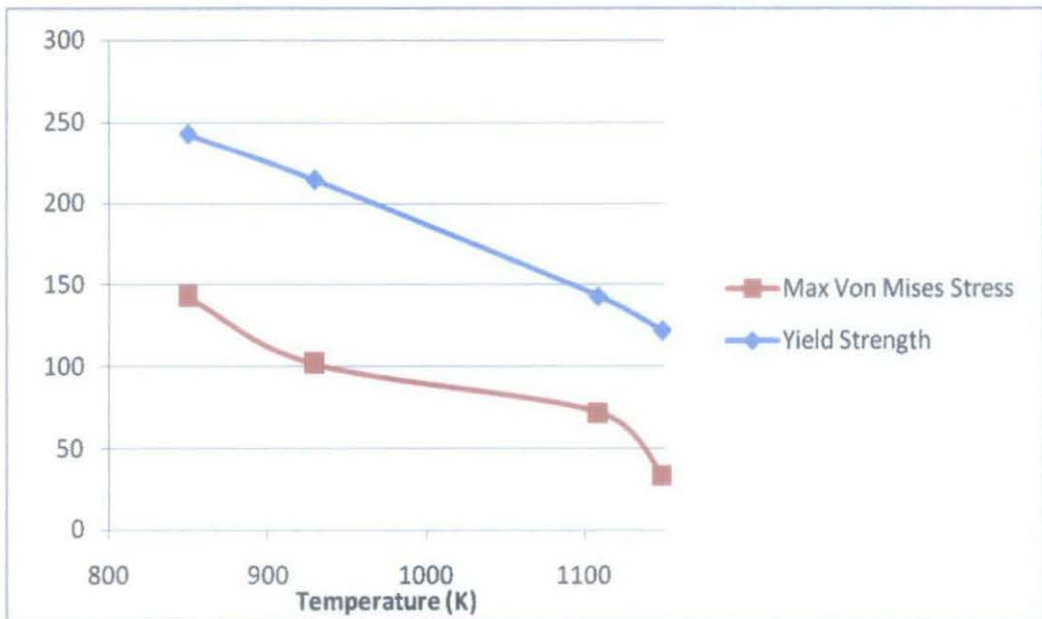


Figure 20: Yield strength and max. Von Mises stress versus temperature

Analyzing table 17 and figure 20 above, none of the von Mises stresses at those define paths exceeded the yield strength of the tube. Thus, the material is able to sustain the load at all locations. However, the possibility of failure is more likely to occur at the region where the process exits and the middle of the tube since the tube has the lowest yield strength at that locations.

CHAPTER 5

CONCLUSION

In this project, the finite element method has been used to analyze thermal stress distribution across a single reformer tube's thickness and length. All the data used in this project referred to a thesis based on a single reformer tube that was retired after 90,000 hours service at Methanex Kitimat plant in British Columbia, Canada. The tube material is Schmidt-Clemens Centralloy® CA4852-Micro centrifugally cast austenitic stainless steel.

The data obtained in ANSYS has been compared with theoretical calculation and seems to agree well with each other. It has been seen that the temperature difference across the tube length resulted from the non-uniform heat transfer coefficient can be considerable causing high thermal stresses. Maximum von mises stress equal to 142.61 MPa developed at the inner surface of the entrance region. The stress then compared with the tensile strength of the tube and it is showed that the tube is able to sustain the stress without fracture.

REFERENCES

- [1] Jones, J and Huber, J. 1997, *Improved Reformer Furnace Efficiency (An Update on Reformer Tube Metallurgy)*, presented at ICI Katalco IMTF97 Conference in San Diego.
- [2] Finite Element Analysis, Simulation and Optimization Method, Retrieved on 14 Feb 2008. *How to Perform a Thermal Stress Analysis?*
<http://www.algor.com/service_support/hints_tips/thermal_stress.asp>
- [3] Bhaumik, S.K., Rangaraju, R., Parameswara, M.A., Bhaskaran, T.A., Venkataswamy, M.A., Raghuram, A.C., and Krishnan, R.V. *Failure of reformer tube of an ammonia plant*. Engineering Failure Analysis, Volume 9, Issue 5, October 2002, P 553-561
<linkinghub.elsevier.com/retrieve/pii/S1350630702000298>.
- [4] R. N. Sinha, Thermal Stress Analysis of Hollow Cylinder by the Finite Element Method. *J. Inst. Engrs (India)* **59** (ME3), 131-133 (1978).
- [5] S.A.R. Naga, Optimum Working Conditions on Thick Walled Cylinders. *J. Engng Mater. Technol. Trans. ASME* 108 (4), 374-376 (1986).
- [6] F.J. Gunha and A. D'Ambra, Cylindrical Component Stress Analysis. *Heat Piping Air Condit.* 59 (11), 96-99 (1987).
- [7] Kandil, A., Analysis of Thick-Walled Cylindrical Pressure Vessels under the Effect of Cyclic Internal Pressure and Cyclic Temperature, *Int. J. Mech. Sci.* Vol. 38, No. 12, pp. 1319-1332, 1996.

- [8] Shariat, M.H., Faraji, A.H., Ashrafiyahy, A. and Alipour, M.M. Retrieved on 9 Feb 2008, <<http://www.jcse.org/Volume6/Preprints/V6Preprint69.pdf>>
- [9] Green, Robert. April 2006. "Re-tubing your primary reformer, *The KATALCOJM PERFORMANCE concept*", 19th AFA Int'l Fertilizer Technical Conference & Exhibition
- [10] Physical Specification of Commonly Cast Heat Resistant Alloys, Retrieved on 13 March 2008, <http://www.alokealloys.com/cast_phy_heat.htm>
- [11] Abdul Wahab, A., Hutchinson, Christopher R. and Kral, Milo V. 2006. *A Three-Dimensional Characterization of Creep Void Formation in Hydrogen Reformer Tubes*, Scripta Materialia 55 (2006) 69-73.
- [12] Brear, J.M., Church, J.M., Humphrey, D.R. and Zanjani, M.S., Life Assessment of Steam Reformer Radiant Catalyst Tube, available online 24 January 2002. <linkinghub.elsevier.com/retrieve/pii/S0308016101001132>
- [13] Widas, Peter. Retrieved on 8 Feb 2008, <http://www.sv.vt.edu/classes/MSE2094_NoteBook/97ClassProj/num/widas/history.html>
- [14] Christensen, P.S., Hansen, V.L., Rostrup-Nielsen, J.R... Synthesis gas production by steam reforming using catalyzed hardware, US Patent Issued on June 8, 2004. <<http://www.patentstorm.us/patents/6746624-description.html>>
- [15] Wikipedia, the free encyclopedia < <http://en.wikipedia.org/wiki> >
- [16] Sundmacher, K., Kienle, A., Seidel-Morgenstem, A.. *Synthesis, Operation, Analysis and Control*, Integrated Chemical Processes, 2006, P9-10.
- [17] Moaveni, Saeed. *Theory and Application with ANSYS*, Finite Element Analysis, Published 1999, P216-234

[18] *Chapter 2, Sequentially Coupled Physics Analysis*, ANSYS Release 9.0
Documentation

[19] Yasar Islamoglu, *Finite element model for thermal analysis of ceramic heat exchanger tube under axial non-uniform convective heat transfer coefficient*, **Materials & Design**, Volume 25, Issue 6, September 2004, Pages 479-482

Appendix I

SELECTED PROPERTIES OF CENTRALLOY CA4852-MICRO

The figures in the following pages represent typical mechanical properties of Schmidt-Clemens Centarlloy CA4852-Micro centrifugal cast tubes. Data for CA4852-Micro were taken from ref [17]. In addition, other physical and mechanical properties are as follows:

Density, $\rho_t = 8000 \text{ kg/m}^3$

Thermal Conductivity, $k_t = 14.6 \text{ W/mK}$

Poisson's ratio, $\nu = 0.3$

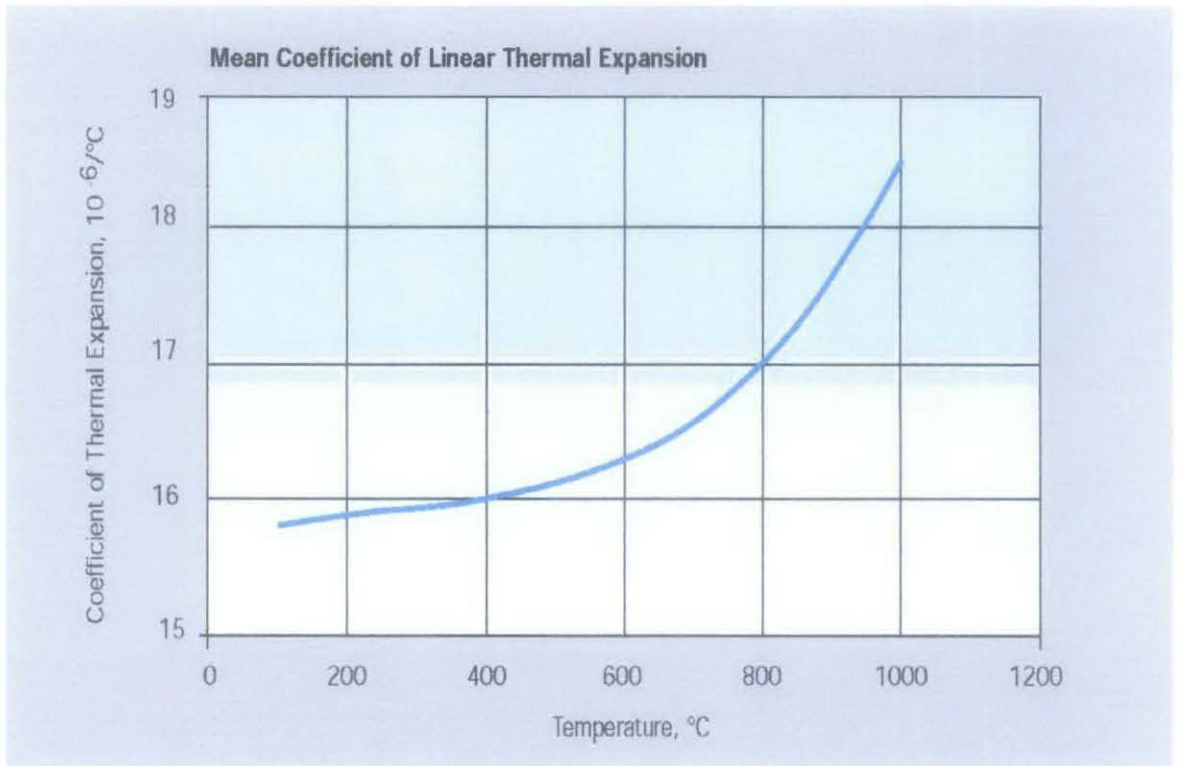


Figure I.1: Coefficient of linear thermal expansion for Schmidt-Clemens Centralloy CA4852-Micro.

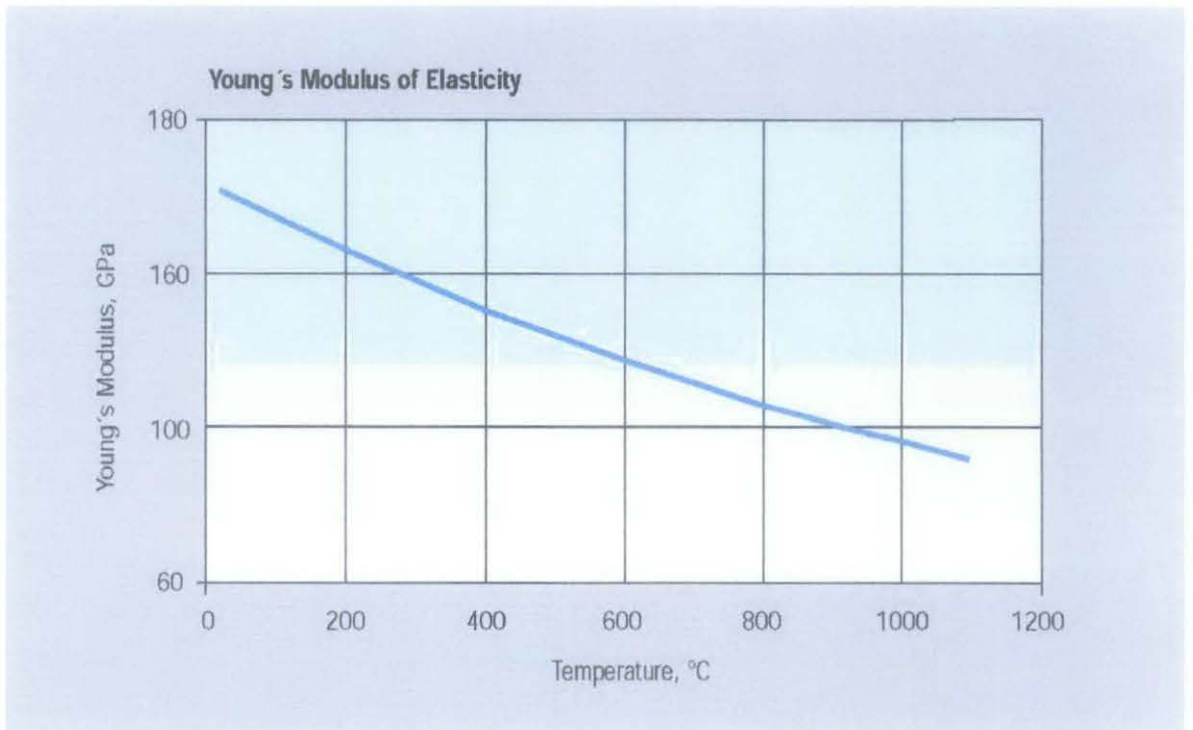
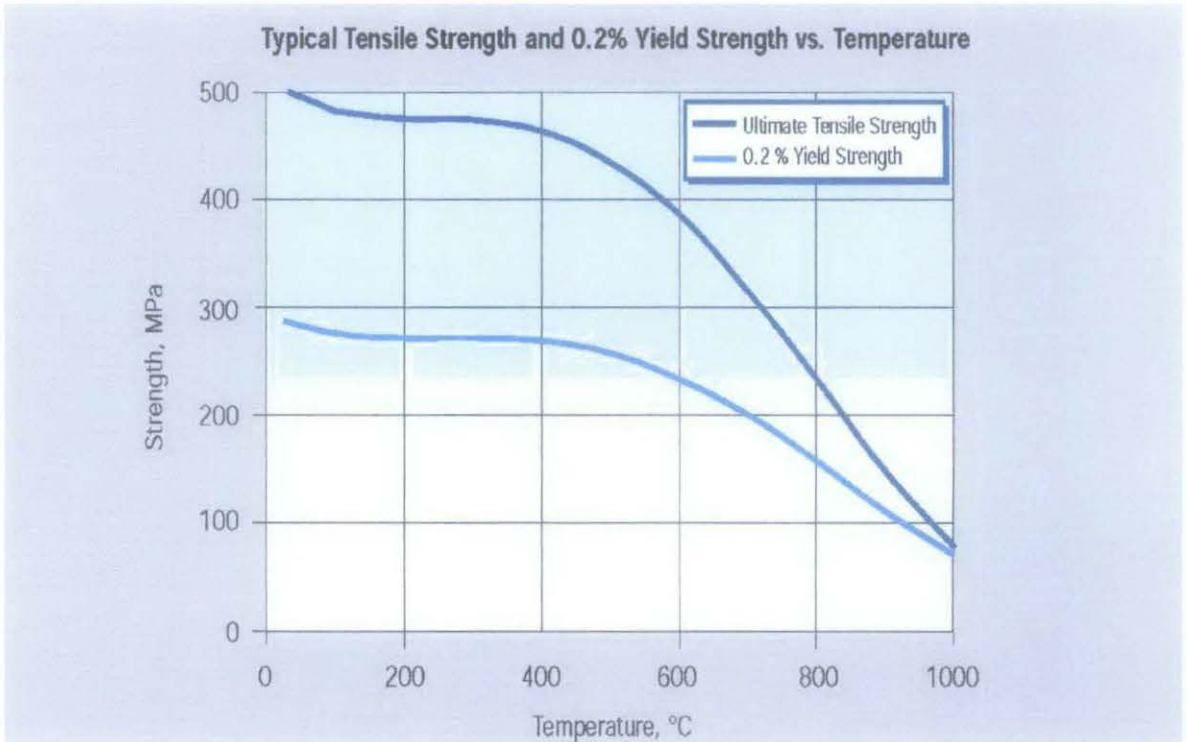
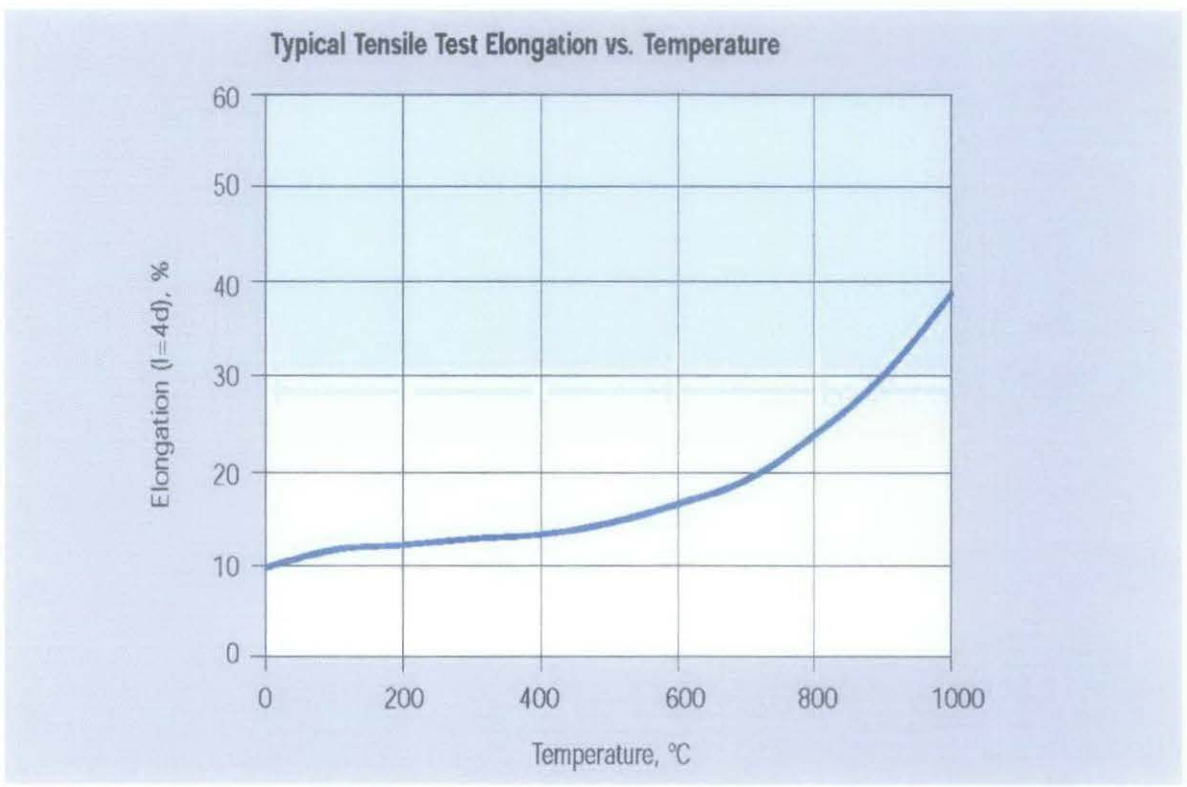


Figure I.2: Modulus of Elasticity for Schmidt-Clemens Centralloy CA4852-Micro.



a) yield and tensile strength;



b) percentage of elongation

Figure I.3: Tensile properties for Schmidt-Clemens Centralloy CA4852-Micro. (a) Yield and tensile strength; (b) percentage of elongation

Appendix II

No.	Detail/ Week	1	2	3	4	5	6	7		8	9	10	11	12	13	14	
1	Selection of Project Topic	■	■						M I D - S E M B R E A K								
2	Research Work on Reformer Tube		■	■	■	■	■	■		■	■	■	■	■	■	■	■
3	Submission of Preliminary Report				●												
4	Find Raw Data for Reformer Tube					■	■	■									
5	Research Work on ANSYS		■	■	■	■	■	■		■	■	■	■	■	■	■	■
5	Model Mechanical and Thermal Loadings Present in the Tube.					■	■	■									
6	Submission of Progress Report										●						
7	Seminar											■	■	■	■		
8	Project work continues										■	■	■	■	■		
9	Submission of Interim Report Final Draft															●	
10	Oral Presentation															●	

● Suggested milestone
 ■ Process

No.	Detail/ Week	1	2	3	4	5	6	7	8	9		11	12	13	14	
1	Prepare batch file for the coupled analysis	■														
2	Submission of progress report 1				●											
3	Verify with theoretical					■										
5	Preparation of poster											■				
6	Poster exposition												●			
7	Preparation of final report											■				
8	Dissertation draft													●		
9	Oral Presentation													●		
10	Hardbound dissertation															●

M
I
D
-
S
E
M

B
R
E
A
K

● Suggested milestone
■ Process

Appendix III

Procedures of using GUI

Define table

1. **Utility Menu > Parameters > Array Parameters > Define/Edit...** The Array Parameters dialog box will appear. Add...chosen.
2. The Add New Array Parameter dialog box appears. "inner" typed in the "Parameter name" field.
3. "Table" selected for parameter array.
4. 24,1 entered as I,J values
5. Y entered as row variable.
6. Click OK.
7. In the Array Parameters dialog box, make sure inner is highlighted and click Edit. The Table Array: INNER=f(Y) table editor dialog box appears.
8. Two columns appear in the table editor dialog box. The first column is column 0; the second column is column 1. Column 0 contains 25 boxes. Do not do anything in the first (top) box. In the five other boxes, the tube's length increment typed. These are row index values.
9. Column 1 also contains 25 boxes. The blue (top) box leave blank. In the other 24 boxes, temperature for every length increment's typed.
10. Choose **File > Apply/Quit**.
11. Close the Array Parameters dialog box.
12. 12. Step 1-11 repeated for outer surface temperature.

Thermal Environment - Create Geometry and Define Thermal Properties

1. **Give example a Title**

Utility Menu > File > Change Title ...
/title, Reformer Tube

2. **Open preprocessor menu**

ANSYS Main Menu > Preprocessor
/PREP7

3. **Create Areas**

Preprocessor > Modeling > Create > Areas > Rectangle > By Dimensions
RECTNG,X1,X2,Y1,Y2

For an axisymmetric problem, ANSYS will rotate the area around the y-axis at x=0.

Table 5: Dimensions of the rectangle created.

X1, X2 X-coordinates	0.125	0.135
Y1, Y2 Y-coordinates	0	12.6

4. **Define the Type of Element**

Preprocessor > Element Type > Add/Edit/Delete...

For this problem the PLANE55 (2-D, Thermal Solid) was used. PLANE55 can be used as a plane element or as an axisymmetric ring element with a 2-D thermal conduction capability. The element has four nodes with a single degree of freedom, temperature, at each node. The element is applicable to a 2-D, steady-state or transient thermal analysis.

5. Turn on Axisymmetry

This was done while the Element Types window is still open by clicking the **Options** button. Axisymmetric was selected under the Element behavior K3.

6. Define Element Material Properties

Preprocessor > Material Props > Material Models > Thermal > Conductivity > Isotropic
In the window that appears, the following geometric properties entered:

i. KXX: 14.6

7. Define Mesh Size

Preprocessor > Meshing > Size Cntrl > ManualSize > Areas > All Areas
Element edge length of 0.0004 was used.

8. Mesh the frame

Preprocessor > Meshing > Mesh > Areas > Free > click 'Pick All'

9. Write Environment

The thermal environment (the geometry and thermal properties) is now fully described and can be written to memory to be used at a later time.
Preprocessor > Physics > Environment > Write

In the window that appears, the TITLE **Thermal** entered.

11. Clear Environment

Preprocessor > Physics > Environment > Clear > OK

Doing this clears all the information prescribed for the geometry, such as the element type, material properties, etc. It does not clear the geometry however, so it can be used in the next stage, which is defining the structural environment.

Structural Environment - Define Physical Properties

Since the geometry of the problem has already been defined in the previous steps, now all that required is to detail the structural variables.

1. Switch Element Type

Preprocessor > Element Type > Switch Elem Type

Thermal to Struc from the scroll down list chosen.

This will switch to the complimentary structural element automatically. In this case it is PLANE 42.

Set plane strain;

Preprocessor > Element Type > Add/Edit/Delete > Options > Element Behavior > Plane strain

2. Define Element Material Properties

Preprocessor > Material Props > Material Models > Structural > Linear > Elastic > Isotropic

In the window that appears, the following geometric properties entered:

IV. Young's Modulus EX:

Table 6: Temperature Dependant, Young Modulus

Temperature	293	473	673	873	1073	1273
EX	170e9	163e9	145e9	127e9	109e9	96e9

ii. Poisson's Ratio PRXY: 0.3

Preprocessor > Material Props > Material Models > Structural > Thermal Expansion Coef > Isotropic

iii. ALPX: 17e-6

3. Write Environment

The structural environment is now fully described.
Preprocessor > Physics > Environment > Write

In the window that appears, the TITLE **Struct** entered.

Solution Phase: Assigning Loads and Solving

4. Define Analysis Type

Solution > Analysis Type > New Analysis > Static
ANTYPE,0

2. Read in the Thermal Environment

Solution > **Unabridged Menu**

Solution > Physics > Environment > Read

Thermal was chosen.

3. Apply Inner Temperature

Solution > Define Loads > Apply > Functions > Define/Edit

Line 4 picked on the pick menu. Select *Existing table* under Apply as and click OK. "inner" table chosen.

4. Apply Outer Temperature

Solution > Define Loads > Apply > Functions > Define/Edit

Pick line 2 in the pick menu. Select *Existing table* under Apply as and click OK. "outer" table chosen.

5. Solve the System

Solution > Solve > Current LS
SOLVE

6. Close the Solution Menu

Main Menu > Finish

It is very important to click **Finish** as it closes that environment and allows a new one to be opened without contamination.

The thermal solution has now been obtained.

7. Read in the Structural Environment

Solution > Physics > Environment > Read

Struct was chosen.

8. Apply Constraints

Solution > Define Loads > Apply > Structural > Displacement > On Lines

Set CP=0 for line 3 and UY=0 for line 1.

9. Apply Pressure

Solution > Define Loads > Setting > For Surface Ld > Gradient

Set; Slope = -33e6, Slope direction = Y

Solution > Define Loads > Apply > Structural > Pressure > On Lines

Line 4 picked and set pressure value = 2.239e6.

10. Include Thermal Effects

Solution > Define Loads > Apply > Structural > Temperature > From Therm Analy

As shown below, the file name File.rth entered. This will couple the results from the solution of the thermal environment to the information prescribed in the structural environment and uses it during the analysis.

11. Define Reference Temperature

Preprocessor > Loads > Define Loads > Settings > Reference Temp

The reference temperature set to 1153 Kelvin.

10. Solve the System

Solution > Solve > Current LS
SOLVE

Appendix IV

Input listing (batch) file

```
Finish
/clear,start
/title, Axisymmetric Tube

*DIM,inner,TABLE,24,1,,Y
INNER(1,0,1)=0
INNER(2,0,1)=0.588
INNER(3,0,1)=1.176
INNER(4,0,1)=1.765
INNER(5,0,1)=2.353
INNER(6,0,1)=2.941
INNER(7,0,1)=3.529
INNER(8,0,1)=4.000
INNER(9,0,1)=4.641
INNER(10,0,1)=5.281
INNER(11,0,1)=5.922
INNER(12,0,1)=6.050
INNER(13,0,1)=6.671
INNER(14,0,1)=7.291
INNER(15,0,1)=7.912
INNER(16,0,1)=8.533
INNER(17,0,1)=9.154
INNER(18,0,1)=9.774
INNER(19,0,1)=10.271
INNER(20,0,1)=10.843
INNER(21,0,1)=11.414
INNER(22,0,1)=11.986
INNER(23,0,1)=12.100
INNER(24,0,1)=12.600
INNER(1,1,1)=849.2
INNER(2,1,1)=923.2
INNER(3,1,1)=986.2
INNER(4,1,1)=1025.5
INNER(5,1,1)=1047.1
INNER(6,1,1)=1062.8
INNER(7,1,1)=1076.5
INNER(8,1,1)=1085.1
INNER(9,1,1)=1093.4
INNER(10,1,1)=1099.6
INNER(11,1,1)=1105.2
INNER(12,1,1)=1106.3
INNER(13,1,1)=1111.8
INNER(14,1,1)=1117.2
INNER(15,1,1)=1122.2
INNER(16,1,1)=1128.2
INNER(17,1,1)=1133.6
INNER(18,1,1)=1138.9
INNER(19,1,1)=1140.6
INNER(20,1,1)=1142.1
INNER(21,1,1)=1145
```

INNER(22,1,1)=1148.4
INNER(23,1,1)=1149
INNER(24,1,1)=1148.9

*DIM,outer, TABLE,24,1,,Y

OUTER(1,0,1)=0
OUTER(2,0,1)=0.588
OUTER(3,0,1)=1.176
OUTER(4,0,1)=1.765
OUTER(5,0,1)=2.353
OUTER(6,0,1)=2.941
OUTER(7,0,1)=3.529
OUTER(8,0,1)=4.000
OUTER(9,0,1)=4.641
OUTER(10,0,1)=5.281
OUTER(11,0,1)=5.922
OUTER(12,0,1)=6.050
OUTER(13,0,1)=6.671
OUTER(14,0,1)=7.291
OUTER(15,0,1)=7.912
OUTER(16,0,1)=8.533
OUTER(17,0,1)=9.154
OUTER(18,0,1)=9.774
OUTER(19,0,1)=10.271
OUTER(20,0,1)=10.843
OUTER(21,0,1)=11.414
OUTER(22,0,1)=11.986
OUTER(23,0,1)=12.100
OUTER(24,0,1)=12.600
OUTER(1,1,1)=929.2
OUTER(2,1,1)=995.9
OUTER(3,1,1)=1055.8
OUTER(4,1,1)=1096.2
OUTER(5,1,1)=1120.1
OUTER(6,1,1)=1135.8
OUTER(7,1,1)=1146.1
OUTER(8,1,1)=1150
OUTER(9,1,1)=1151
OUTER(10,1,1)=1150.1
OUTER(11,1,1)=1149.2
OUTER(12,1,1)=1149.1
OUTER(13,1,1)=1149.2
OUTER(14,1,1)=1150
OUTER(15,1,1)=1151.5
OUTER(16,1,1)=1153.5
OUTER(17,1,1)=1155.9
OUTER(18,1,1)=1158.4
OUTER(19,1,1)=1156.8
OUTER(20,1,1)=1155.1
OUTER(21,1,1)=1156.3
OUTER(22,1,1)=1158.5
OUTER(23,1,1)=1159
OUTER(24,1,1)=1158.9

/prep7

jobname ='reformer tube'

!MODELLING OF GEOMETRY

```
rectng,0.125,0.135,0,12.6 ! Create rectangle
et,1,55 ! Define element type
keyopt,1,3,1 ! Turns on axisymmetry
mp,kxx,1,14.6 ! Thermal conductivity
mp,dens,1,8000 ! Define density

eshape,2
esize,0.0004 ! Mesh size
amesh,all ! Mesh the area

seltol, 0.000001
lsel,s,line,,4
dl,all,,temp,%INNER%,1
lsel,s,line,,2
dl,all,,temp,%OUTER%,1
lsel,all
physics,write,thermal ! Write physics environment as thermal
physics,clear ! Clear the environment

etchg,tts ! Switch element type
et,1,42
keyopt,1,3,1
mptemp,1,293,473,673,873,1073,1273,1373 !Kelvin, seven temperatures
mpdata,ex,1,1,170e9,163e9,145e9,127e9,109e9,96e9 !N/m^2
mpdata,prxy,1,1,0.3,0.3,0.3,0.3,0.3,0.3 !Poisson's ratio
mptemp,1,373,473,673,873,1073,1273
mpdata,alpx,1,1,1.57e-5,1.58e-5,1.6e-5,1.63e-5,1.7e-5,1.85e-5 !Expansion coefficient

seltol, 0.000001
allsel
nset,s,loc,y,12.6 ! To simulate Generalize plane strain - free to expand
cp,1,uy,all ! Coupling to force to a set of node to have same DOF value
nset,s,loc,y,0
d,all,uy,0
nset,all
/pnum, line, 1 ! Turn on Line number

sfgrad,pres,0,y,0,- 33261.9 ! Define pressure gradient
nset,s,loc,x,0.125
sf,all,pres,2.239e6
allsel
physics,write,struct ! Write physics environment as struct
save
finish

/solu ! Enter the solution phase
antype,0 ! Steady-state analysis
physics,read,thermal ! Read in the thermal environment
sfran
sbctran
solve
finish
```

```

/solu                                ! Re-enter the solution phase
physics,read,struct                  ! Read in the struct environment
ldread,temp,,,,,,,,rth               ! Apply loads derived from thermal environment
tref,1153
SFTRAN                                ! Transfer solid model to FE model
SBCTRAN                               ! Transfer BC to FE model
seltol
solve
finish

/post1
PATH,bottom,2,,                      ! Define path with name
PPATH,1,,0.125,0,0                   ! Define path points
PPATH,2,,0.135,0,0
pdef,U_X,U,X
pdef,S_X,S,X
pdef,S_Y,S,Y
pdef,S_Z,S,Z
pdef,S_EQV,S,EQV
prpath,XG,U_X,S_X,S_Y,S_Z,S_EQV     ! List the stress solution
plpath,XG,U_X,S_X,S_Y,S_Z,S_EQV

PATH,inner,2,63,                     ! Define path with name
PPATH,1,,0.125,0,0                   ! Define path points
PPATH,2,,0.125,12.6,0
pdef,U_X,U,X
pdef,S_X,S,X
pdef,S_Y,S,Y
pdef,S_Z,S,Z
pdef,S_EQV,S,EQV
prpath,XG,U_X,S_X,S_Y,S_Z,S_EQV     ! List the stress solution
plpath,XG,U_X,S_X,S_Y,S_Z,S_EQV

```

Appendix V

Sample calculation at the inner surface of the entrance region with:

Inner temperature: 849.2 K

Outer temperature: 929.2 K

Pressure: 2.239×10^6

Radius, r : 0.125 m

III.I Thermal Stresses

S_X, radial stress:

$$\sigma_{rr} = \frac{a_T E (T_i - T_o)}{2(1-\nu)} \left[\frac{-\ln r_o/r + \left(\frac{r_o}{r}\right)^2 - 1}{\ln r_o/r_i + \left(\frac{r_o}{r_i}\right)^2 - 1} \right]$$
$$\sigma_{rr} = \frac{(17 \times 10^{-6})(118 \times 10^9)(849.2 - 929.2)}{2(1-0.3)} \left[\frac{-\ln(0.135/0.125) + \left(\frac{0.135}{0.125}\right)^2 - 1}{\ln(0.135/0.125) + \left(\frac{0.135}{0.125}\right)^2 - 1} \right]$$
$$= 0$$

S_Y, axial stress:

$$\sigma_{ax} = \frac{a_T E (T_i - T_o)}{2(1-\nu)} \left[\frac{1 - 2 \ln r_o/r}{\ln r_o/r_i + \left(\frac{r_o}{r_i}\right)^2 - 1} - \frac{2}{\left(\frac{r_o}{r_i}\right)^2 - 1} \right]$$
$$\sigma_{ax} = \frac{(17 \times 10^{-6})(118 \times 10^9)(849.2 - 929.2)}{2(1-0.3)} \left[\frac{1 - 2 \ln(0.135/0.125)}{\ln(0.135/0.125) + \left(\frac{0.135}{0.125}\right)^2 - 1} - \frac{2}{\left(\frac{0.135}{0.125}\right)^2 - 1} \right]$$
$$= 117.568 \text{ MPa}$$

S_Z, hoop stress:

$$\sigma_{hr} = \frac{\alpha_T E (T_i - T_o)}{2(1-\nu)} \left[\frac{1 - \ln\left(\frac{r_o}{r}\right) - \left(\frac{r_o}{r}\right)^2 + 1}{\ln\left(\frac{r_o}{r_i}\right) - \left(\frac{r_o}{r_i}\right)^2 - 1} \right]$$
$$\sigma_{hr} = \frac{(17 \times 10^{-6})(118 \times 10^9)(849.2 - 929.2)}{2(1-0.3)} \left[\frac{1 - \ln\left(\frac{0.135}{0.125}\right) - \left(\frac{0.135}{0.125}\right)^2 + 1}{\ln\left(\frac{0.135}{0.125}\right) - \left(\frac{0.135}{0.125}\right)^2 - 1} \right]$$
$$= 117.568 \text{ MPa}$$

III.II Stresses Due to Internal Pressure

S_X, radial stress:

$$\sigma_{rp} = \frac{pr_i^2}{r_o^2 - r_i^2} \left[1 - \frac{r_o^2}{r^2} \right]$$
$$\sigma_{rp} = \frac{(2.234 \times 10^6)(0.125)^2}{0.135^2 - 0.125^2} \left[1 - \frac{0.135^2}{0.125^2} \right]$$
$$= -0.224 \text{ MPa}$$

S_Y, axial stress:

Assume 0 (generalized plane strain condition)

S_Z, hoop stress:

$$\sigma_{hp} = \frac{pr^2}{r_o^2 - r^2} \left[1 + \frac{r_o^2}{r^2} \right]$$
$$\sigma_{hp} = \frac{(2.234 \times 10^6)(0.125)^2}{0.135^2 - 0.125^2} \left[1 + \frac{0.135^2}{0.125^2} \right]$$
$$= 29.122 \text{ Mpa}$$

To determine Von Mises stress,

$$\begin{aligned}\sigma_1 &= \sigma_{hT} + \sigma_{hp} \\ &= 117.568 \text{ MPa} + 29.122 \text{ MPa} \\ &= 146.69 \text{ MPa}\end{aligned}$$

$$\begin{aligned}\sigma_2 &= \sigma_{rT} + \sigma_{rp} \\ &= 0 - 0.224 \text{ MPa} \\ &= -0.224 \text{ MPa}\end{aligned}$$

$$\begin{aligned}\sigma_3 &= \sigma_{aT} + \sigma_{ap} \\ &= 117.568 \text{ MPa} + 0 \text{ MPa} \\ &= 117.568 \text{ MPa}\end{aligned}$$

$$\begin{aligned}\text{Von Mises, } \bar{\sigma}_H &= \frac{1}{\sqrt{2}} \sqrt{(\sigma_1 - \sigma_2)^2 + (\sigma_2 - \sigma_3)^2 + (\sigma_3 - \sigma_1)^2} \\ &= \frac{1}{\sqrt{2}} \sqrt{(146.69 - 0.224)^2 + (-0.224 - 117.568)^2 + (117.568 - 146.69)^2} \\ &= 190.198 \text{ MPa}\end{aligned}$$

Appendix VI

Theoretical results

IV.I Stresses across the tube's thickness at entrance region.

radius	radial,Sx	axial,Sy	hoop,Sz	Seqv
0.125	-2.23900E+06	1.17568E+08	1.46718E+08	1.36733E+08
0.1255	-1.67040E+06	1.05676E+08	1.34258E+08	1.24130E+08
0.126	-1.15556E+06	9.38319E+07	1.21899E+08	1.11697E+08
0.1265	-6.93440E+05	8.20344E+07	1.09639E+08	9.94462E+07
0.127	-2.83032E+05	7.02834E+07	9.74775E+07	8.73964E+07
0.1275	7.66547E+04	5.85785E+07	8.54130E+07	7.55806E+07
0.128	3.86592E+05	4.69195E+07	7.34440E+07	6.40556E+07
0.1285	6.47729E+05	3.53060E+07	6.15693E+07	5.29263E+07
0.129	8.60997E+05	2.37375E+07	4.97876E+07	4.24014E+07
0.1295	1.02731E+06	1.22138E+07	3.80976E+07	3.29341E+07
0.13	1.14755E+06	7.34542E+05	2.64981E+07	2.55595E+07
0.1305	1.22260E+06	-1.07007E+07	1.49878E+07	2.22659E+07
0.131	1.25331E+06	-2.20922E+07	3.56557E+06	2.45833E+07
0.1315	1.24053E+06	-3.34403E+07	-7.76975E+06	3.11682E+07
0.132	1.18506E+06	-4.47453E+07	-1.90193E+07	3.98726E+07
0.1325	1.08773E+06	-5.60076E+07	-3.01843E+07	4.95210E+07
0.133	9.49307E+05	-6.72275E+07	-4.12657E+07	5.95995E+07
0.1335	7.70576E+05	-7.84052E+07	-5.22648E+07	6.98745E+07
0.134	5.52289E+05	-8.95412E+07	-6.31825E+07	8.02301E+07
0.1345	2.95188E+05	-1.00636E+08	-7.40199E+07	9.06040E+07
0.135	0.00000E+00	-1.11689E+08	-8.47780E+07	1.00960E+08

IV.II Stresses distribution across the tube's thickness in the middle of the tube's length

radius	radial,Sx	axial,Sy	hoop,Sz	Seqv
0.125	-2.02900E+06	5.29380E+07	7.93540E+07	7.19110E+07
0.1255	-1.71607E+06	4.75835E+07	7.36865E+07	6.63226E+07
0.126	-1.42802E+06	4.22502E+07	6.80652E+07	6.08421E+07
0.1265	-1.16438E+06	3.69381E+07	6.24895E+07	5.54819E+07
0.127	-9.24676E+05	3.16469E+07	5.69586E+07	5.02596E+07
0.1275	-7.08455E+05	2.63765E+07	5.14720E+07	4.52005E+07
0.128	-5.15270E+05	2.11267E+07	4.60290E+07	4.03415E+07
0.1285	-3.44684E+05	1.58974E+07	4.06291E+07	3.57373E+07
0.129	-1.96267E+05	1.06884E+07	3.52717E+07	3.14706E+07
0.1295	-6.95995E+04	5.49959E+06	2.99562E+07	2.76649E+07
0.13	3.57286E+04	3.30746E+05	2.46820E+07	2.45001E+07
0.1305	1.20120E+05	-4.81825E+06	1.94486E+07	2.22133E+07
0.131	1.83970E+05	-9.94757E+06	1.42555E+07	2.10528E+07
0.1315	2.27664E+05	-1.50573E+07	9.10202E+06	2.11667E+07
0.132	2.51580E+05	-2.01477E+07	3.98772E+06	2.25012E+07
0.1325	2.56090E+05	-2.52188E+07	-1.08792E+06	2.48302E+07
0.133	2.41557E+05	-3.02709E+07	-6.12542E+06	2.78797E+07
0.1335	2.08336E+05	-3.53040E+07	-1.11253E+07	3.14180E+07
0.134	1.56776E+05	-4.03182E+07	-1.60880E+07	3.52790E+07
0.1345	8.72190E+04	-4.53138E+07	-2.10140E+07	3.93510E+07
0.135	0.00000E+00	-5.02909E+07	-2.59038E+07	4.35598E+07

IV.III Stress distribution across the tube's thickness at the exit region.

radius	radial,Sx	axial,Sy	hoop,Sz	Seqv
0.125	-1.81990E+06	1.32015E+07	3.68952E+07	3.38075E+07
0.1255	-1.66862E+06	1.18662E+07	3.54086E+07	3.24974E+07
0.126	-1.52442E+06	1.05362E+07	3.39344E+07	3.12271E+07
0.1265	-1.38716E+06	9.21149E+06	3.24724E+07	2.99990E+07
0.127	-1.25671E+06	7.89199E+06	3.10225E+07	2.88155E+07
0.1275	-1.13295E+06	6.57768E+06	2.95844E+07	2.76796E+07
0.128	-1.01575E+06	5.26851E+06	2.81581E+07	2.65945E+07
0.1285	-9.04989E+05	3.96444E+06	2.67432E+07	2.55637E+07
0.129	-8.00549E+05	2.66544E+06	2.53398E+07	2.45912E+07
0.1295	-7.02313E+05	1.37147E+06	2.39476E+07	2.36812E+07
0.13	-6.10165E+05	8.24804E+04	2.25664E+07	2.28382E+07
0.1305	-5.23994E+05	-1.20156E+06	2.11962E+07	2.20668E+07
0.131	-4.43690E+05	-2.48069E+06	1.98368E+07	2.13719E+07
0.1315	-3.69146E+05	-3.75495E+06	1.84880E+07	2.07582E+07
0.132	-3.00255E+05	-5.02437E+06	1.71497E+07	2.02300E+07
0.1325	-2.36915E+05	-6.28899E+06	1.58217E+07	1.97913E+07
0.133	-1.79024E+05	-7.54885E+06	1.45040E+07	1.94452E+07
0.1335	-1.26484E+05	-8.80398E+06	1.31963E+07	1.91939E+07
0.134	-7.91961E+04	-1.00544E+07	1.18986E+07	1.90382E+07
0.1345	-3.70660E+04	-1.13002E+07	1.06107E+07	1.89779E+07
0.135	0.00000E+00	-1.25414E+07	9.33244E+06	1.90111E+07

IV.IV Stress distribution on the inner surface across the tube's length

Distance from entrance	radial,Sx	axial,Sy	hoop,Sz	Seqv
0.000	-2.23900E+06	1.17568E+08	1.46690E+08	1.36714E+08
0.588	-2.21944E+06	1.06840E+08	1.35708E+08	1.25998E+08
1.176	-2.19989E+06	1.02284E+08	1.30898E+08	1.21348E+08
1.765	-2.18030E+06	1.03901E+08	1.32259E+08	1.22742E+08
2.353	-2.16074E+06	1.07281E+08	1.35385E+08	1.25869E+08
2.941	-2.14118E+06	1.07281E+08	1.35131E+08	1.25683E+08
3.529	-2.12163E+06	1.02284E+08	1.29880E+08	1.20595E+08
4.000	-2.10596E+06	9.53771E+07	1.22769E+08	1.13681E+08
4.641	-2.08464E+06	8.46490E+07	1.11763E+08	1.03003E+08
5.281	-2.06336E+06	7.42148E+07	1.01052E+08	9.26592E+07
5.922	-2.04204E+06	6.46624E+07	9.12227E+07	8.32263E+07
6.050	-2.03778E+06	6.28989E+07	8.94038E+07	8.14888E+07
6.050	-2.03778E+06	6.28989E+07	8.94038E+07	8.14888E+07
6.671	-2.01713E+06	5.49631E+07	8.11993E+07	7.36887E+07
7.291	-1.99651E+06	4.82029E+07	7.41709E+07	6.70664E+07
7.912	-1.97585E+06	4.21775E+07	6.78769E+07	6.11939E+07
8.533	-1.95520E+06	3.71809E+07	6.26116E+07	5.63348E+07
9.154	-1.93454E+06	3.27721E+07	5.79342E+07	5.20670E+07
9.774	-1.91392E+06	2.86572E+07	5.35511E+07	4.81179E+07
10.271	-1.89739E+06	2.58650E+07	5.05438E+07	4.54416E+07
10.271	-1.89739E+06	2.38075E+07	4.84864E+07	4.36367E+07
10.843	-1.87837E+06	1.91048E+07	4.35362E+07	3.93680E+07
11.414	-1.85938E+06	1.66065E+07	4.07909E+07	3.70467E+07
11.986	-1.84035E+06	1.48430E+07	3.87799E+07	3.53647E+07
12.100	-1.83656E+06	1.46960E+07	3.85837E+07	3.51976E+07
12.600	-1.81993E+06	1.47254E+07	3.83968E+07	3.50105E+07

IV.V Stress distribution on the outer surface across the tube's length

Distance from entrance	radial,Sx	axial,Sy	hoop,Sz	Seqv
0.000	0	-1.11689E+08	-8.48039E+07	1.00968E+08
0.588	0	-1.01497E+08	-7.48471E+07	9.11429E+07
1.176	0	-9.71695E+07	-7.07540E+07	8.70225E+07
1.765	0	-9.87052E+07	-7.25249E+07	8.85663E+07
2.353	0	-1.01916E+08	-7.59708E+07	9.17378E+07
2.941	0	-1.01916E+08	-7.62056E+07	9.18021E+07
3.529	0	-9.71695E+07	-7.16937E+07	8.72666E+07
4.000	0	-9.06078E+07	-6.53200E+07	8.09813E+07
4.000	0	-9.06078E+07	-6.53200E+07	8.09813E+07
4.641	0	-8.04161E+07	-5.53844E+07	7.12768E+07
5.281	0	-7.05037E+07	-4.57276E+07	6.19502E+07
5.922	0	-6.14290E+07	-3.69088E+07	5.35585E+07
6.050	0	-5.97537E+07	-3.52846E+07	5.20300E+07
6.050	0	-5.97537E+07	-3.52846E+07	5.20300E+07
6.671	0	-5.22146E+07	-2.79936E+07	4.52585E+07
7.291	0	-4.57925E+07	-2.18191E+07	3.96721E+07
7.912	0	-4.00685E+07	-1.63430E+07	3.48961E+07
8.533	0	-3.53217E+07	-1.18443E+07	3.11376E+07
9.154	0	-3.11333E+07	-7.90393E+06	2.80300E+07
9.774	0	-2.72242E+07	-4.24242E+06	2.53704E+07
10.271	0	-2.45716E+07	-1.78829E+06	2.37280E+07
10.271	0	-2.26170E+07	1.66265E+05	2.27006E+07
10.843	0	-1.81495E+07	4.40539E+06	2.07067E+07
11.414	0	-1.57761E+07	6.55075E+06	1.98782E+07
11.986	0	-1.41007E+07	7.99764E+06	1.93795E+07
12.100	0	-1.39611E+07	8.09173E+06	1.93225E+07
12.600	0	-1.39891E+07	7.86412E+06	1.91716E+07